Report as of FY2007 for 2007GA155B: "Quantifying the Precipitation-Stream-Aquifer System Response in the Lower Apalachicola-Chattahoochee-Flint (ACF) River Basin"

Publications

Project 2007GA155B has resulted in no reported publications as of FY2007.

Report Follows

QUANTIFYING THE PRECIPITATION-STREAM-AQUIFER SYSTEM RESPONSE IN THE LOWER APALACHICOLA-CHATTAHOOCHEE-FLINT (ACF) RIVER BASIN

By Jian Luo

School of Civil and Environmental Engineering

Georgia Institute of Technology

Atlanta, GA 30332-0355

Georgia Water Resources Institute Report

April 30, 2008

CONTENTS

FIGURES

TABLES

QUANTIFYING THE PRECIPITATION-STREAM-AQUIFER SYSTEM RESPONSE IN THE LOWER APALACHICOLA-CHATTAHOOCHEE-FLINT (ACF) RIVER BASIN

by Jian Luo

ABSTRACT

Groundwater is the major water source in the lower Apalachicola-Chattahoochee-Flint (ACF) River basin in southwestern Georgia. The long-term sustainability of groundwater resources in the basin has been threatened by the increased demand of groundwater withdrawals in recent decades and drought conditions. The research project aims to conduct quantitative analyses to improve our understanding of the correlations in the precipitation-stream-aquifer system in the basin, which will ultimately help develop proactive and rational monitoring and management plans to ensure the long-term sustainability of groundwater resources.

Multivariate geostatistical methods based on variogram models are applied to investigate the joint spatial and temporal correlations and variations of groundwater level, streamflow, precipitation, and groundwater withdrawal. The variogram models that are applied include stationary and nonstationary models, and separable and nonseparable models. Characteristic space scales and timescales or fractal characteristics are identified. Kriging systems using identified variogram models are used for spatiotemporal data mapping and forecasting.

Results and benefits of the research project include: (1) quantitative descriptions of the spatiotemporal correlations in the precipitation-stream-aquifer system; (2) characteristic spatial scales and timescales for sampling design and data interpretation; (3) predictions of groundwater levels and streamflow in different scenarios; and (4) guidelines and tools, such as software, that can assist in the decision-making for water resources management in southwestern Georgia.

INTRODUCTION

Groundwater withdrawals for farm irrigation have increased dramatically in recent decades, especially in the lower Apalachicola-Chattahoochee-Flint (ACF) River basin in southwestern Georgia [*Leeth et al.*, 2005]. By 1995, agriculture used about 722 million gallons per day (Mgal/d) of water, of which about 66 percent (479 Mgal/d) was groundwater [*Fanning*, 1997]. During the 2002 drought year, agriculture used 42 percent (1285 Mgal/d) of the total water use in Georgia, with about 60 percent (745 Mgal/d) of irrigation water extracted from the groundwater flow system [*Fanning*, 2003]. Previous studies have indicated groundwater withdrawals in the ACF River basin have lowered the water level in the Upper Floridan aquifer, the main water-bearing aquifer in Southwest Georgia, and resulted in significantly reduced streamflow, adversely impacting downstream users. In addition, drought conditions from the early to mid-1980s and from 1998 to 2002 also caused noticeable declining trends in groundwater levels. Furthermore, due to budget cuts for the operation and maintenance of the real-time monitoring network, the Georgia Geological Survey is planning to discontinue several real-time monitoring stations. There is thus an imperative need to understand the implications of the increased groundwater stresses within the context of the existing institutional constraints and develop proactive and rational monitoring and management plans to ensure the long-term sustainability of the Georgia surface water and groundwater resources.

To this end, a good understanding of the correlations in the precipitation-stream-aquifer system is critical for (1) designing a reliable monitoring network in southwestern Georgia and (2) using the network information to effectively predict the response of the stream-aquifer system and formulate sound water resources planning and management policies. Equally critical is the understanding of the increased water resources stresses on groundwater quality. The proposed research project aims to conduct quantitative analyses of relationships among groundwater levels, precipitation, streamflow, and groundwater quality.

The US and Georgia Geological Surveys routinely collect data and perform numerical simulation and statistical analyses. However, the proposed work has not been carried out before and is needed for several important reasons:

- The presence of both spatial and temporal heterogeneities in the surface-subsurface water system complicates the scientific analyses and decision making, be it through theoretical studies, field measurements, or model developments.

- The relations among precipitation, streamflow, groundwater levels, and groundwater quality exhibit complex correlations and variations in space, requiring a plethora of spatial data to resolve the properties of these relations.

- The variability may occur over scales differing by many orders of magnitude, from local irrigation areas up to the basinwide flow system, and from individual rain events up to seasonal rain fluctuations.

Purpose and Scope

In this report, we systematically address the issues mentioned above by applying multivariate geostatistical methods to space-time data analyses. These analyses aim to identify the correlations and variations of the above-mentioned variables and to examine the existence of characteristic scales in both space and time. Furthermore, our study will advance the development of the scientific theory and methodology for the space-time data analysis in hydrology, which may be applicable for effective water resources management in Georgia and elsewhere. The study relied on data from published data by USGS. Specific objectives include:

- To develop and critically evaluate broad, general principles and approaches of multivariate geostatistical analyses for hydrologic data in time and space.

- To examine the main variables (precipitation, groundwater level, streamflow, and groundwater quality) jointly in space and time and estimate spatio-temporal correlation models.

- To estimate characteristic scales both in space and time for the main variables in the lower ACF River basin or, alternatively, identify their fractal characteristics.

- To analyze the effects of groundwater withdrawal on the precipitation-stream-aquifer system both in space and time.

- To generate historical and forecasting maps of the groundwater level, quality and seepage in terms of groundwater withdrawal and precipitation.

- To develop a set of tools and outlines for effective water resources management for the lower ACF River basin.

Description of Study Area

The 6,800 –mi^2 study area in the lower ACF River basin is shared by southeastern Alabama, northwestern Florida, and southwestern Georgia (Fig. 1A). The Apalachicola drains from Lake Seminole across the Florida Panhandle and flows into the Gulf of Mexico. The Chattahoochee begins in north Georgia, flows out of Lake Lanier, forms the border between Alabama and Georgia, and flows into Lake Seminole in the extreme southwest corner of the state. Lastly, the Flint begins just south of Atlanta and merges with Chattahoochee in Lake Seminole. The lower ACF River Basin is drained by all of the three rivers and their tributaries [*Torak et al.*, 1996]. Six major aquifers underlie the ACF River basin. In the lower ACF River basin, the highly permeable, karstic Upper Floridan aquifer is the major source of groundwater supply (Fig. 1B) [*Torak et al.*, 1996]. The physiography, hydrogeologic setting, surface- and ground-water hydrology, and climate in the study area have been described in the USGS reports [*Torak et al.*, 1996; *Mosner*, 2002; *Albertson and Torak*, 2002]. The characteristics are summarized as follows:

- The Upper Floridan aquifer is unconfined or semiconfined, connected to surface-water bodies by springflow and seepage through the extremely productive Ocala Limestone and younger units, the main water-bearing unit of the Upper Floridan aquifer.

- Aquifer thickness and hydraulic conductivity of the Upper Floridan aquifer are spatially heterogeneous.

- The groundwater level in the Upper Floridan aquifer fluctuates considerably in response to climate change, infiltrated precipitation, groundwater withdrawal, evaporation, and discharge to surface-water bodies.

- Precipitation is one of the primary mechanisms in recharging both surface- and ground-waters in this area.

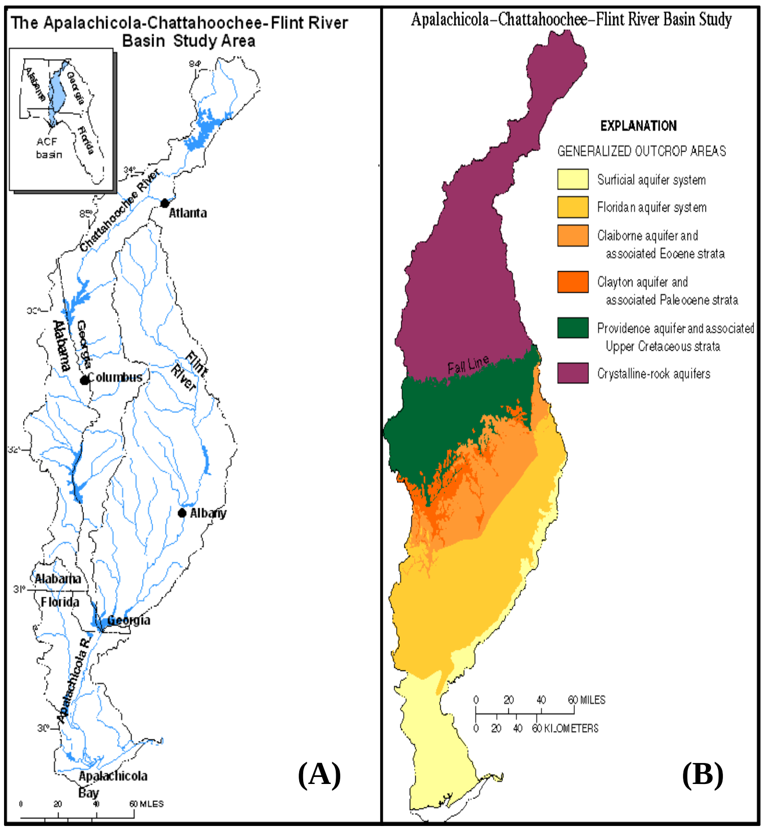

Figure 1 (A) ACF River basin location map; and (B) The aquifers in the ACF River basin [USGS, http://ga.water.usgs.gov/nawqa/main.maps.html].

These characteristics cannot be conveniently incorporated into a groundwater model to simulate the hydrologic cycling in the lower ACF River basin. Previous investigations of this area were mostly focused on the evaluation of the hydrogeologic conditions and water resources potential [e.g., *Torak et al.*, 1993, 1996; *Torak and McDowell*, 1996; *Torak and Painter*, 2006]. *Albertson* [2001], *Mosner* [2002], *Torak* [2001], and *Warner and Lawrence* [2005] discussed the hydrogeology, water chemistry, and stream-aquifer relations in the lower ACF River basin. However, the spatio-temporal correlations and variations were not explored, and multivariate analyses were not considered for important variables: precipitation, groundwater level, streamflow rate, and groundwater quality. *Torak et al.* [1996], *Torak and McDowell* [1996], and *Albertson and Torak* [2002] developed two-dimensional steady-state models to study the effect of groundwater pumpage on stream-aquifer flow in the lower ACF River basin. These deterministic models involved solutions of the governing flow equations of modeling piezometric head levels in the aquifer. However, such deterministic models typically require a large number of input parameters that are not convenient to determine, such as the hydraulic conductivity field, precipitation infiltration, and initial and boundary conditions, etc. In the absence of understanding the spatial and temporal relations in the precipitation-stream-aquifer system, models, technologies and strategies that could potentially optimize the water use cannot be translated successfully into practice.

Data Description

Most of the data used in this research plan stem from the comprehensive hydrographic data sets measured by the monitoring system in Georgia and reported by annual hydrologic summaries and literatures. The “Georgia HydroWatch” system consists of 223 real-time monitoring stations, which provide real-time water-stage data, with streamflow computed at 198 locations, and rainfall recorded at 187 stations [*USGS Fact Sheet*, 2006a]. Fig. 2A shows the map of the USGS streamflow monitoring network, more than 80 percent of which include precipitation gages [*USGS Fact Sheet*, 2006a]. The USGS groundwater network for Georgia currently consists of 170 wells for continuous monitoring groundwater levels and qualities. Figure 2B shows the location of the monitoring wells. In particular, there are a larger number of monitoring wells in our study area in southwestern Georgia, where there are issues of groundwater withdrawal [*USGS Fact Sheet*, 2006b].

Water use data has been collected by the Georgia Water-Use Program (GWUP), a cooperative program between the USGS and the GaEPD, annually since 1980 and published in a state report every fifth year.

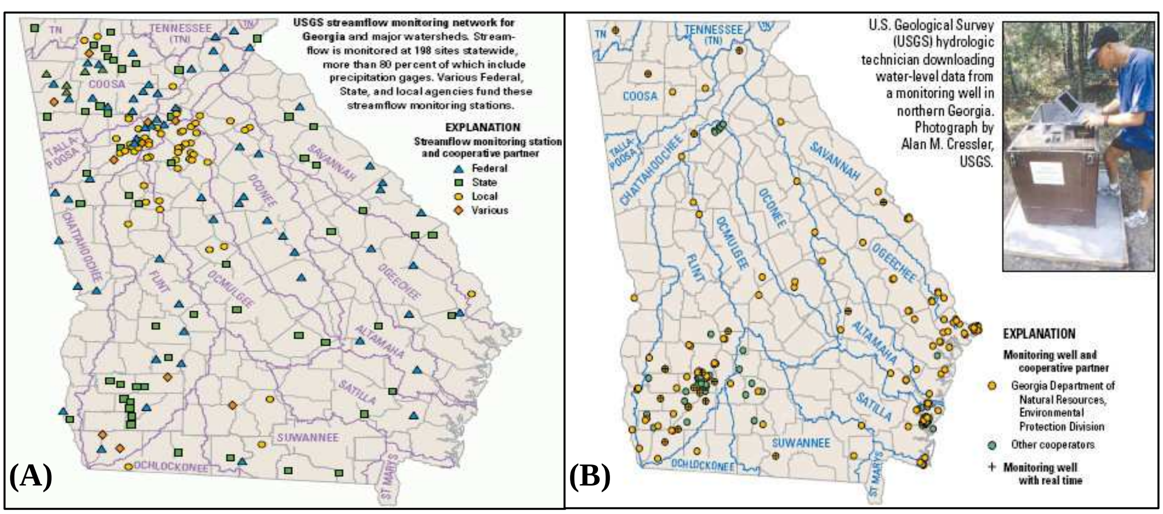

Figure 2 (A) The USGS streamflow monitoring network for Georgia [*USGS Fact Sheet*, 2006a]; and (B) The USGS groundwater monitoring network for Georgia [*USGS Fact Sheet*, 2006b].

Table 1 summarizes the data series that may be available for the geostatistical analyses. The numbers of stations in the lower ACF River basin is less than the listed numbers. We will focus on the data collected in the area of interest, and we will also consider other monitoring stations to examine the scale issue. The aggregate information of groundwater use data will be used by assuming a spatially homogeneous process. Furthermore, groundwater level measurements also indicate effects of groundwater withdrawals. Geostatistical space-time models have been also developed for addressing the difference between scales regarding the original and aggregate processes [*Rodrguez-Iturbe and Meja*, 1974; *Solna and Switzer*, 1996].

Table 1. Data Series Available for Analyses

Data Type	Size	Number of Stations	Time Resolution	Period
Groundwater level	Point	170	Monthly average and real time	Current conditions; 2000-2005 and historical data
Streamflow	Point	198	Monthly average and real time	Current conditions; 2000-2005 and historical data
Precipitation	Point	187	Monthly average and real time	Current conditions; 2000-2005 and historical data
Grounewater quality	Point	170	Monthly average and real time	Current conditions; 2000-2005 and historical data
Groundwater use	Regional	160 Counties	Yearly	1980-2000

Methods of Study

Geostatistical spatio-temporal models are considered as alternative approaches when elaborate physically based models are unavailable. The statistical framework complements the analysis for space-time data that relies on the joint spatial and temporal dependence between observations. In addition, stochastic models, built on some patterns of the observed spatio-temporal variability, are based typically on a small number of parameters that can be inferred and modeled, without necessarily following the underlying governing equations [*Cressie*, 1993; *Wackernagel*, 1995; *Kitanidis*, 1997; *Kyriakidis and Journel*, 1999]. Furthermore, geostatistical spatio-temporal models may also be related to physically based models through the trend component of stochastic models and the residuals between the observations and deterministically predicted values [*Christakos and Raghu*, 1996; *Jones and Zhang*, 1997; *Venkatram*, 1988; *Haslett*, 1989; *Pereira et al.*, 1997; *Haas*, 1998].

The challenges to analyze space-time data include:

- The units and scales of space-time data are different and cannot be directly compared in a physical sense.

- There has been a lack of known valid models for space-time covariances and variograms.

Because of the intrinsic ordering and nonreversibility, temporal data cannot be simply treated as spatial data. For example, the definition of isotropy in space has no meaning for temporal data. Therefore, space--time data were traditionally analyzed independently through models initially developed for spatial or temporal distributions. For instance, to compare the properties in the spatial patterns over time, spatial analyses, instead of joint space-time analyses, may be applied to study the attributes of interest over specific time instants [*Tabios and Salas,* 1985; *Goovaerts and Chiang*, 1993; *Simard and Marcotte*, 1993; *Hudson and Wackernagel*, 1994]. Alternatively, at specific locations, temporal analyses may be applied to study time series data. The joint space-time dependence may be analyzed based on the independent spatial or temporal models by correlating the model parameters in time or space [e.g., *Bras and Rodrigues-Iturbe*, 1983; *Cressie*, 1993]. The concept of anisotropy may be employed to analyze space-time data, i.e., time is considered as an additional space dimension with a different scale. This treatment makes it straightforward to conveniently apply all the developed spatial models. *Myers and Journel* [1990] and *Rouhani and Myers* [1990] discussed the difficulties associated with this method.

Two types of covariance and variogram models, for describing correlations and variabilities of space-time data, may be available: (1) separable models; and (2) nonseparable models. A spatial-temporal random field $Z(\mathbf{x},t)$, where $\mathbf{x}$ represents spatial location and t time, is separable if $\mathrm{Cov}\left[Z(\mathbf{x},t),Z(\mathbf{x}',t')\right]=C_s(\mathbf{x},\mathbf{x}')C_t(t,t')$ for some spatial covariance C_s and temporal covariance C_t [*De Cesare et al.*, 1997; *Posa*, 1993; *Rodriguez-Iturbe and Mejia*, 1974]. Nonseparable models have also been generated to describe space-time data [*Cressie and Huang*, 1999; *De Iaco et al.*, 2001; *Gneiting*, 2002; *Stein*, 2003]. The separable model represents the random field as a combination of independent components in separate domains, yielding factorized or separable covariance and nested structure variogram which allow treating space and time separately by techniques developed and successfully used in time series analyses and geostatistics. Separability is desirable because it decreases computational efforts dramatically, but it is usually a rather unrealistic assumption for large spatial-temporal domains.

The covariance and variogram models can also be divided into stationary and nonstationary models. For stationary models, characteristic scales may be defined when the variogram flattens out. For nonstationary variables, fractal characteristics may be identified if variograms increase as a power of distance, indicating long term persistence or large spatial correlations [*Klemes*, 1974; *Kirchner et al.*, 2000]. With characteristic scales, one can adopt one typical length and time to represent a particular process instead of dealing with a spectrum of lengths and times. It is therefore useful to investigate whether characteristic scales or fractal characteristics exist.

Finally, the estimated covariance and variogram models can be used to generate realization or best estimates using kriging systems. Both historical and forecasting maps can be obtained to serve as the input functions and calibrations for a groundwater model.

Acknowledgment

The author extends thanks to the support from Georgia Water Resources Institute and the Director Dr. Georgakakos. Without their help and guidance, completion of the study would have been more difficult and technically incomplete.

Thanks are extended to J. Davis, and A. Tidwell for their management support. The author also is grateful to Younghun Jung, Ana Maria Hagan, and Chia-Jeng Chen for help in developing, organizing, and analyzing the project data base. Younghun Jung conducted spatial analysis for streamflow rate, groundwater level, and precipitation using an optimal searching method for identifying the optimal spatial correlations; Chia-Jeng Chen conducted spatiotemporal analysis for precipitation by describing the mean function as a Fourier type function and analyzing the spatial distribution of the parameters of the mean function; and Ana Maria Hagan conducted the spatiotemporal analysis of the groundwater withdraw data in the ACF river basin, and the covariance analysis between groundwater withdraw, irrigation depths and groundwater levels.

SPATIAL CORRELATIONS OF STREAMFLOW, GROUNDWATER LEVEL, AND PRECIPITATION

Model

The spatial correlation is generally represented by semi-variogram. The experimental spatial semi-variogram at a certain time can be calculated as the average of the spatial variograms of the observations in time:

$$\hat{\gamma}_s(h_s) = \frac{1}{\sum_{i=1}^{N_t} 2n_i(h_s)} \sum_{i=1}^{N_t} \sum_{j=1}^{n_i(h_s)} \left[Z(\mathbf{x}_j + h_s, t_i) - Z(\mathbf{x}_j, t_i)\right]^2 \tag{1}$$

where h_s is the space lag, $Z(\mathbf{x}_j, t_i)$ is the value of the random variable at time t_i and spatial location $\mathbf{x}_j$ of station j , N_t is the number of time steps, and $n_i(h_s)$ is the number of pairs with space lag h_s .

Data Treatment

The USGS Georgia monitoring network provides 14 stations for recording groundwater level and precipitation during 2005 and 2006, and 22 stations for streamflow rate. Each data group is daily measurement. Yearly averages are analyzed by Eq. (1). Figure 3A-C shows the spatial distribution and the magnitude of these measurements in ACF river basin. Larger precipitation is found in the southern basin than in the northern basin. In addition, the streamflow rate increased exponentially along the main stream, and the flint river tributaries have lower individual streamflow rates.

Locations of all monitoring stations are provided in the units of longitude and latitude. The Haversine formula is applied to calculate the distance between two stations. For two points on a sphere (of radius R) with latitudes φ_1 and φ_2, latitude separation $\Delta\varphi = \varphi_1 - \varphi_2$, and longitude separation $\Delta\lambda$, where angles are in radians, the spherical distance d between the two points (along a great circle of the sphere) can be related to their locations by the formula

$$haver\sin\left(\frac{d}{R}\right) = haver\sin(\Delta\varphi) + \cos(\varphi_1)\cos(\varphi_2) haver\sin(\Delta\lambda) \tag{2}$$

Let h denote haversin(d/R), given from above. The spherical distance can be evaluated by:

$$d = R \cdot haver\sin^{-1}(h) = 2R\arcsin\left(\sqrt{h}\right) \tag{3}$$

Model Validation

The criterion to validate the semi-variogram model is the Q_1 and Q_2 tests based on statistical principles for kriging residuals. Q_1 is defined as the sample mean of kriging residuals, and Q_2 is the sample mean of squared errors of kriging residuals. Ideally, Q_1 should be near 0, and Q_2 should be close to 1. In addition, the optimal semi-variogram model is given by minimizing the estimation variance:

$$cR = Q_2 \exp\left(\frac{1}{n-1}\sum_{i=2}^{n}\ln\left(\sigma_i^2\right)\right) \tag{4}$$

subject to

$$Q_2 = 1 \tag{5}$$

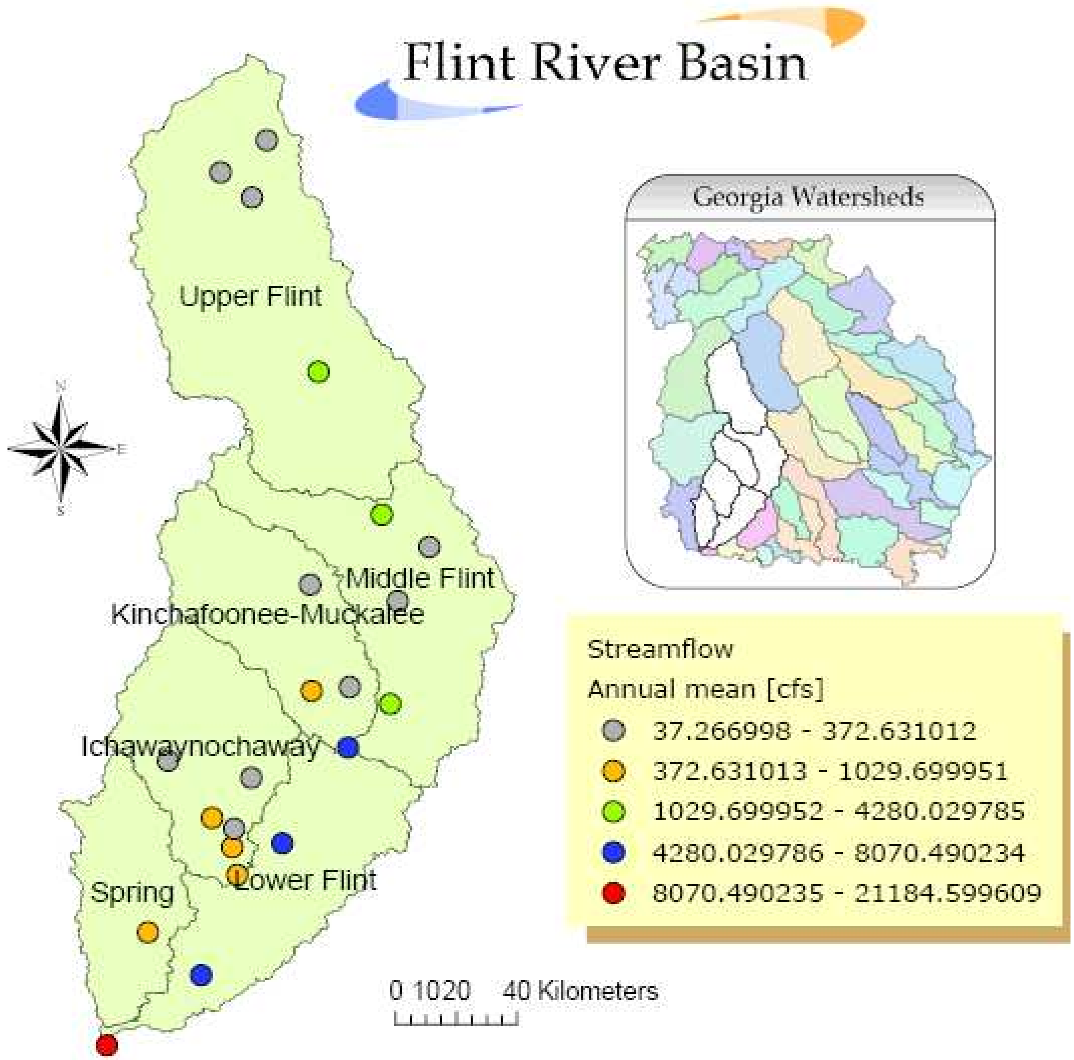

Figure 3. (A) Spatial distribution of the streamflow rate in the Flint River Basin.

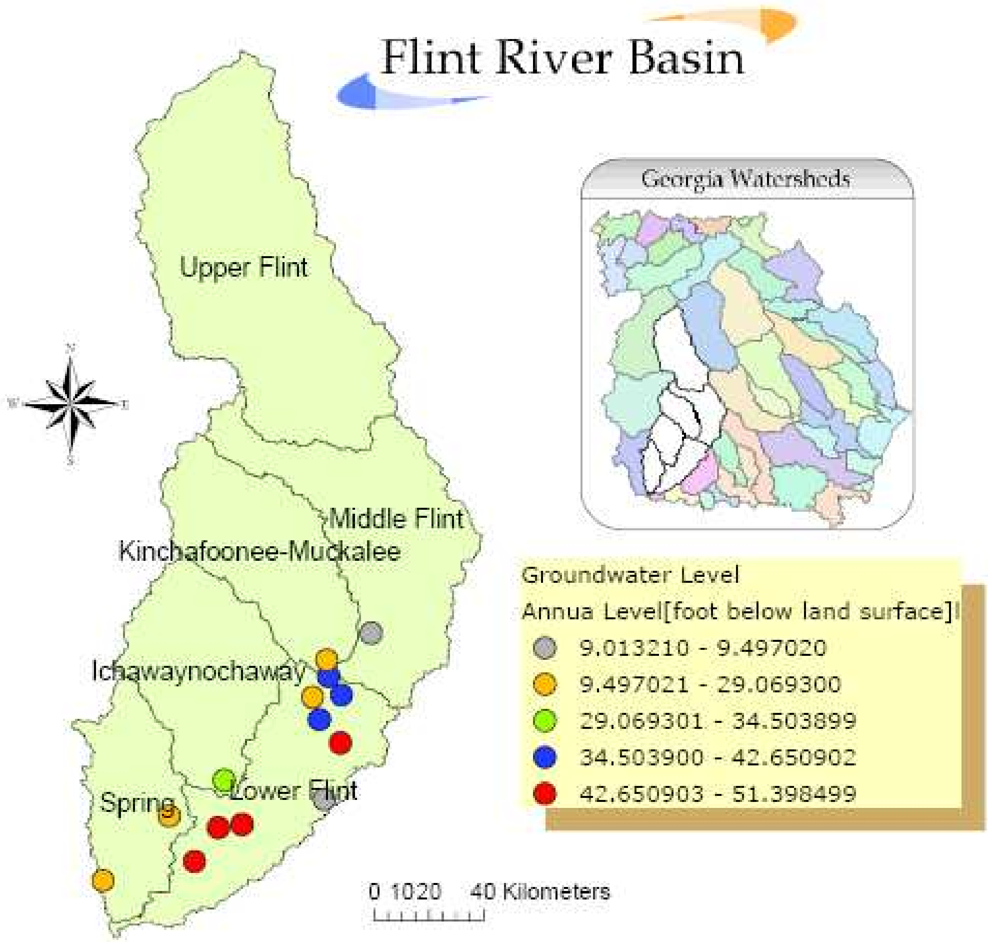

Figure 3. (B) Spatial distribution of the groundwater level in the Flint River Basin.

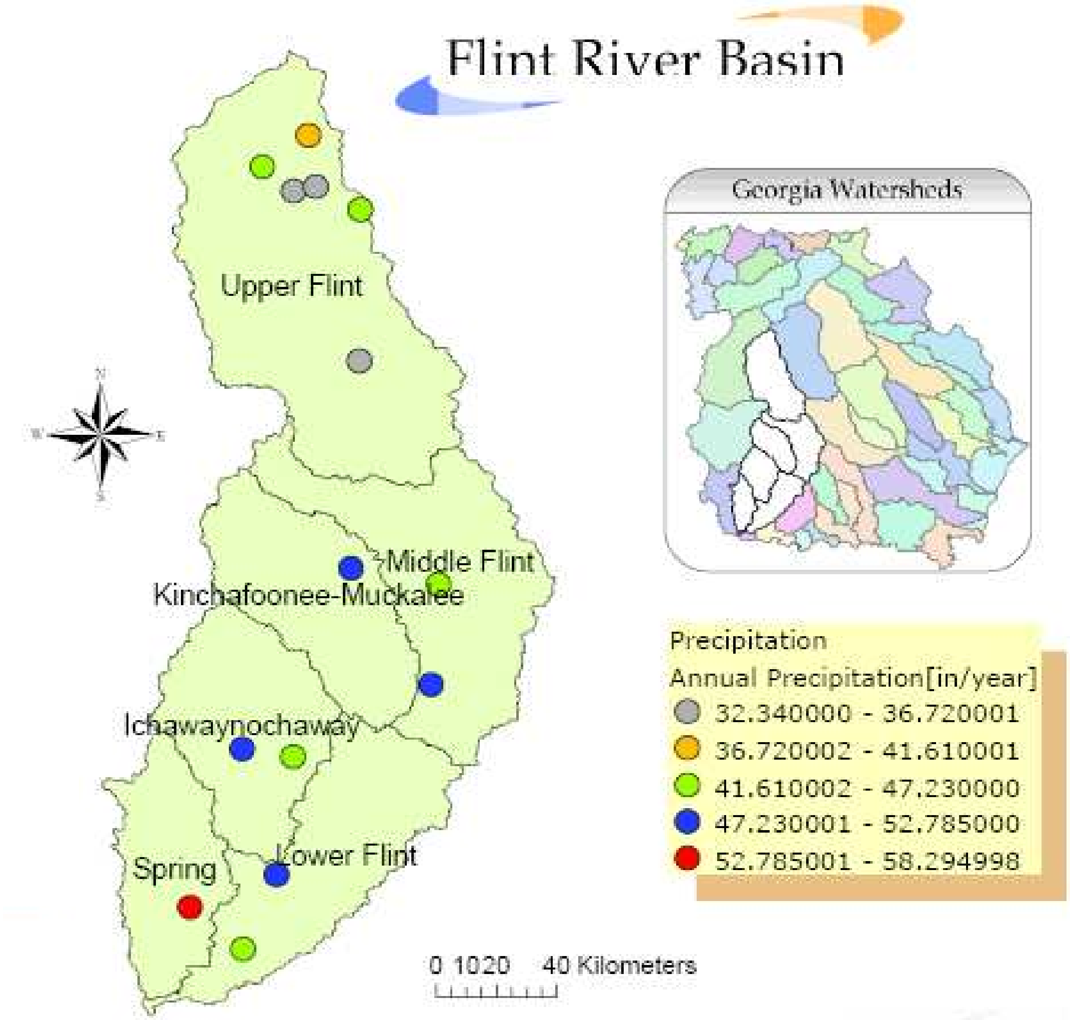

Figure 3. (C) Spatial distribution of the precipitation in the Flint River Basin.

Table 2 summarizes the optimal coefficients of exponential semi-variogram models for describing spatial correlations of streamflow rate, groundwater level, and precipitation. The nugget effect is applied in case that microscale correlations cannot be identified by the current monitoring network. The correlation range is about 3 times of the integral length for an exponential model. Thus, the spatial correlation ranges are 10.7, 0.4, and 25.5km for streamflow rate, groundwater level, and precipitation, respectively.

Table 2. The optimal values with minimum *cR* subject to $|Q_2\text{-}1|<0.01$

	Streamflow	Groundwater level	Precipitation
σ^2	192.6798	242.6702	152.6799
L	3.5655	0.1381	8.4985
Nugget	0	0	35.6833
Q1	-0.36118	-0.06979	-0.035333
Q2	1.01	1.01	1.01
cR	16.3716	206.9507	55.492

Figures 4A-6A show the raw, experimental variogram and the semi-variogram models that pass the Q_1 and Q_2 tests and the optimal models. Figures 4B-6B and 4C-6C show the distributions of the coefficients as a function of *cR*.

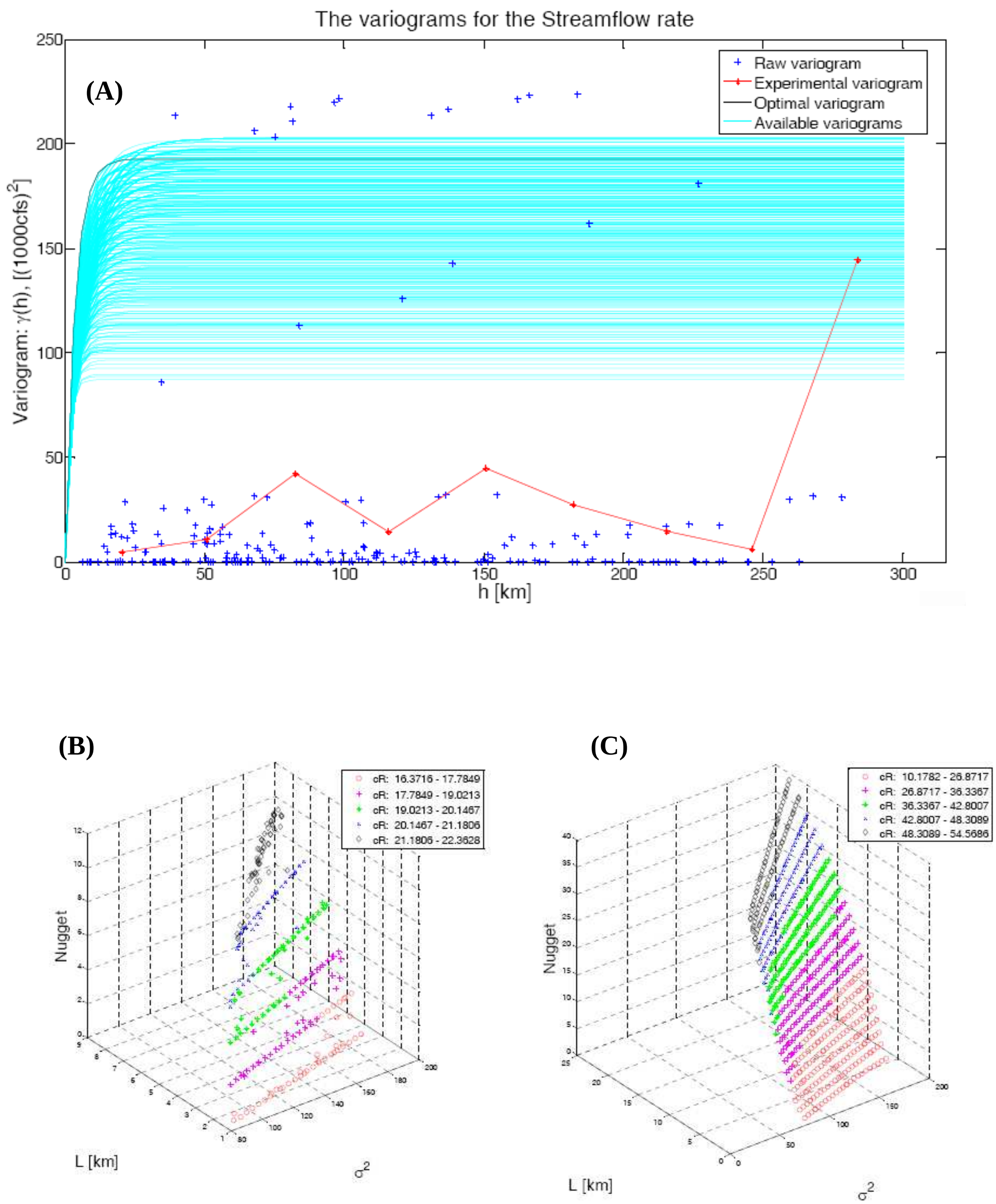

Figure 4. Semi-variogram model estimation for streamflow rate. (A) raw and experimental variogram and semi-variogram models pass Q_1 and Q_2 tests; (B) distribution of coefficients; (C) distribution of coefficients.

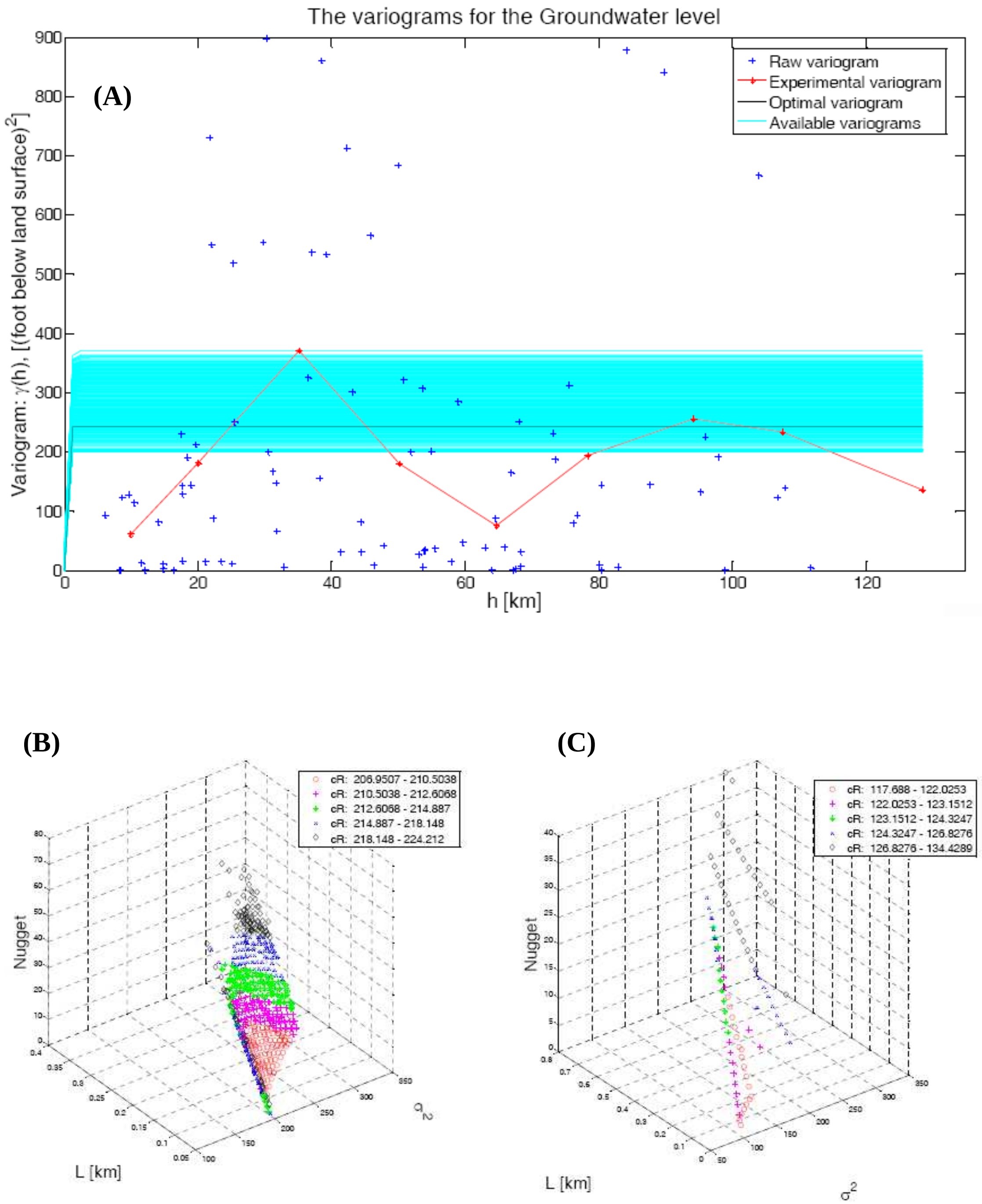

Figure 5. Semi-variogram model estimation for streamflow rate. (A) raw and experimental variogram and semi-variogram models pass Q_1 and Q_2 tests; (B) distribution of coefficients; (C) distribution of coefficients.

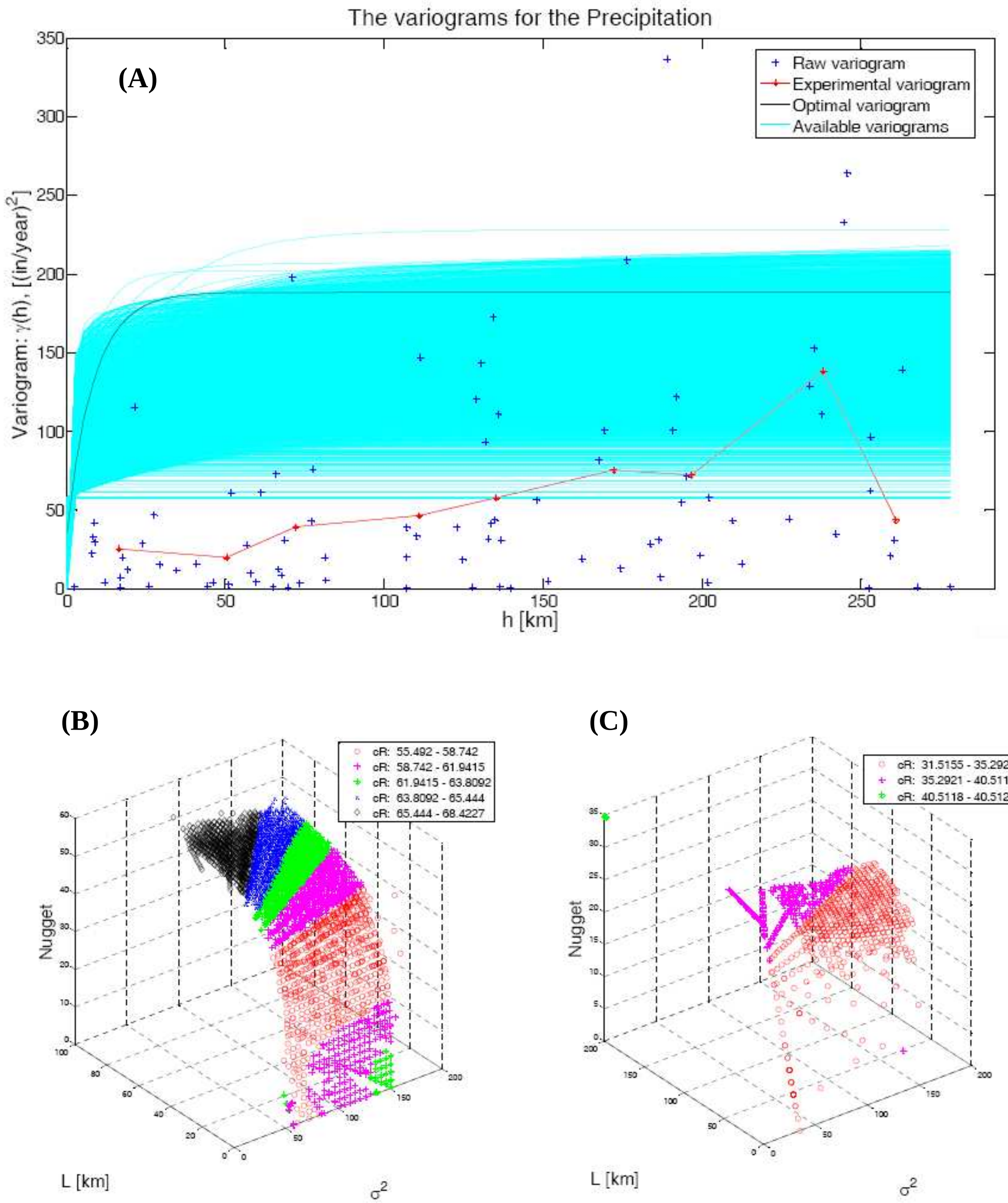

Figure 6. Semi-variogram model estimation for streamflow rate. (A) raw and experimental variogram and semi-variogram models pass Q_1 and Q_2 tests; (B) distribution of coefficients; (C) distribution of coefficients.

SPATIOTEMPORAL ANALYSIS OF PRECIPITATION

Model

The experimental temporal variograms can be calculated as the average of the temporal variograms of the individual time series:

$$\hat{\gamma}_t(h_t) = \frac{1}{\sum_{j=1}^{N_s} 2n_j(h_t)} \sum_{j=1}^{N_s} \sum_{i=1}^{n_j(h_t)} \left[Z(\mathbf{x}_j, t_i + h_t) - Z(\mathbf{x}_j, t_i) \right]^2 \tag{6}$$

where h_t is the time lag, $Z(\mathbf{x}_j, t_i)$ is the value of the transformed variable at time t_i and spatial location $\mathbf{x}_j$ of station j, N_s is the number of data series, and $n_j(h_t)$ is the number of pairs with time lag h_t.

The experimental spatial-temporal variogram can be evaluated by:

$$\hat{\gamma}_{st}(h_s, h_t) = \frac{1}{\sum_{j=1}^{N_t(h_s)} 2n_j(h_t)} \sum_{j=1}^{N_s(h_s)} \sum_{i=1}^{n_j(h_t)} \left[Z(\mathbf{x}_j + h_s, t_i + h_t) - Z(\mathbf{x}_j, t_i) \right]^2 \tag{7}$$

Saptiotemporal data can be analyzed by the vectorial time series approach and the single spatiotemporal random function approach. The difference is that the latter approach only considers the data from previous time events. This is more suitable for real-time estimation and forecasting.

Mean Function

Mean function for precipitation is estimated by monthly data measured by the Georgia monitoring network (Figure 7). The essential mean function is described by a Fourier type function, and no obvious trend is observed (Figure 8).

$$m(x,t) = b_0(x)\cos\left(\frac{\pi}{6}t\right) + b_1(x)\sin\left(\frac{\pi}{6}t\right) \tag{8}$$

Spatial Correlation and Random Field Generation

The mean function has two factors, b0 and b1, which are considered as spatial random functions. The semi-variogram analysis is presented by Figures 9 and 10 for each of them. Best linear estimations of spatial distributions of these two factors are obtained by ordinary kriging systems. Periodic precipitation generation can also be done by assuming independent Gaussian random fields for factors 1 and 2 (Figure 11).

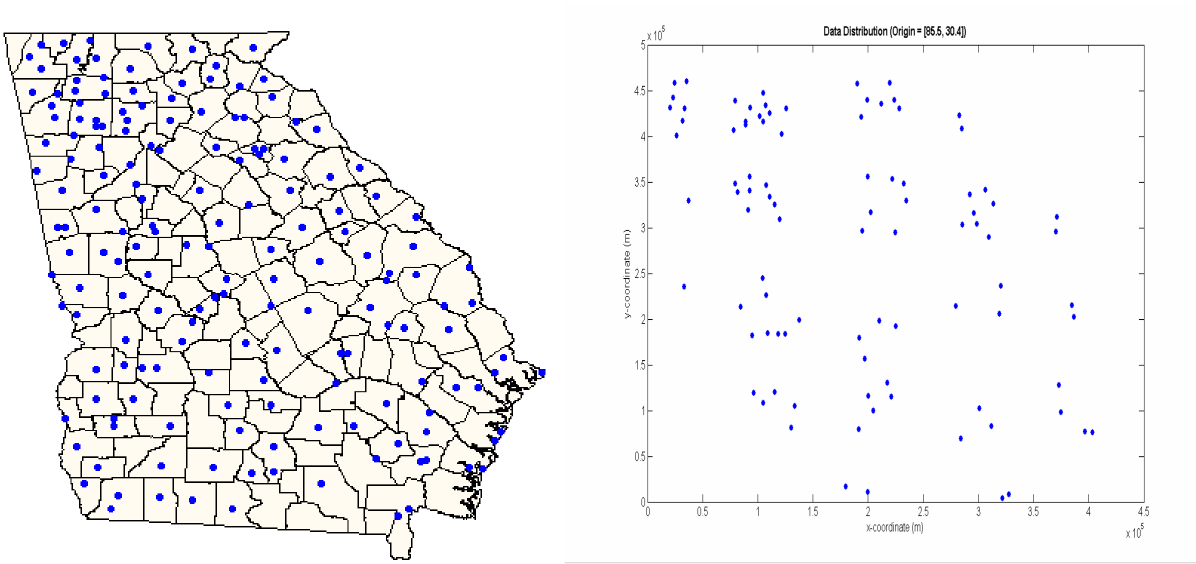

Figure 7. Monitoring system for precipitation in Georgia.

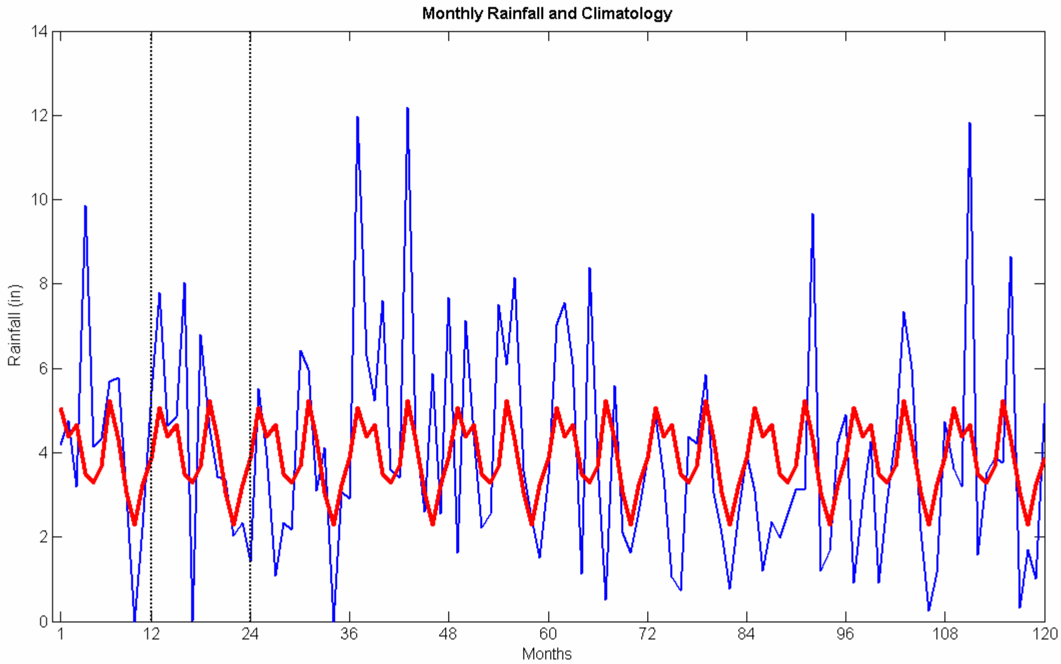

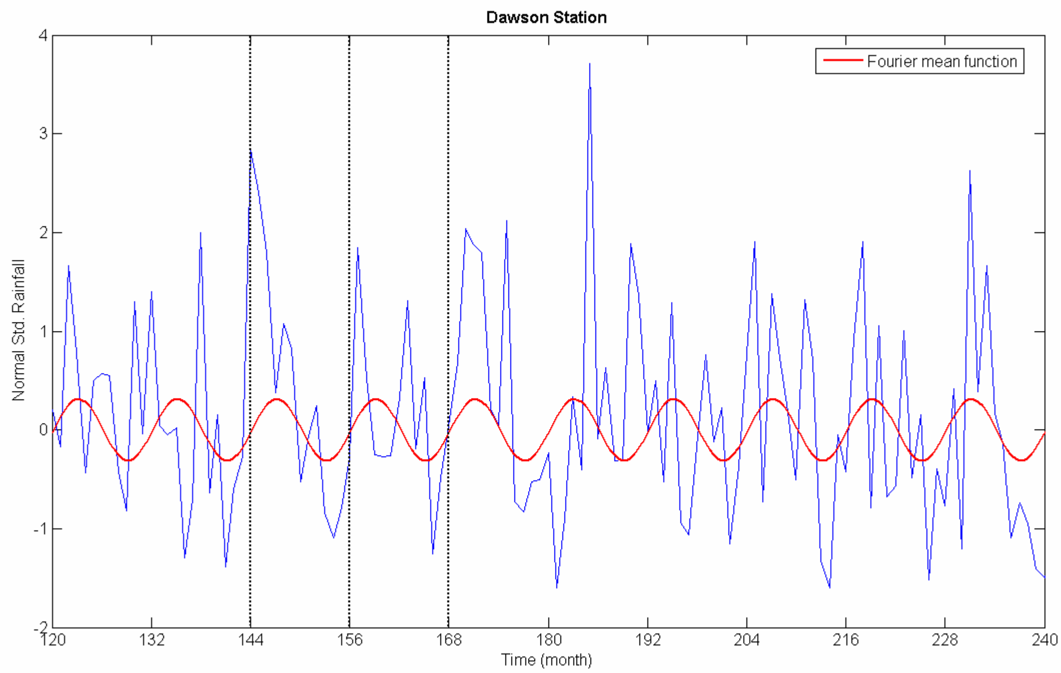

Figure 8. Mean function of precipitation. No trend is observed.

(A)

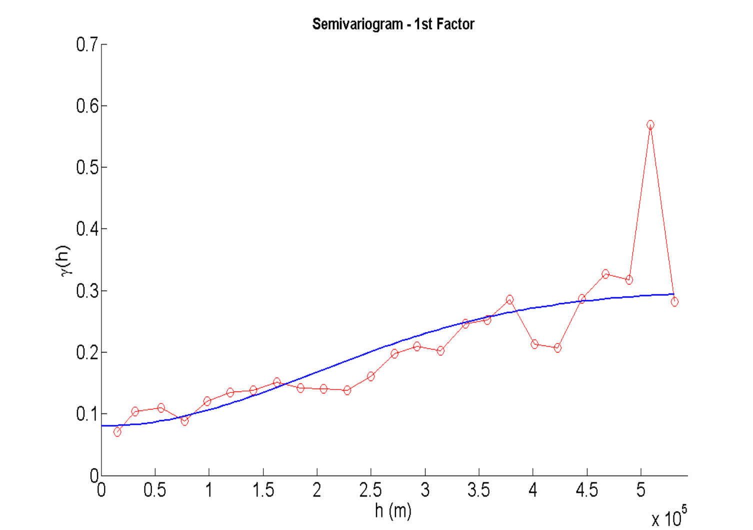

(B)

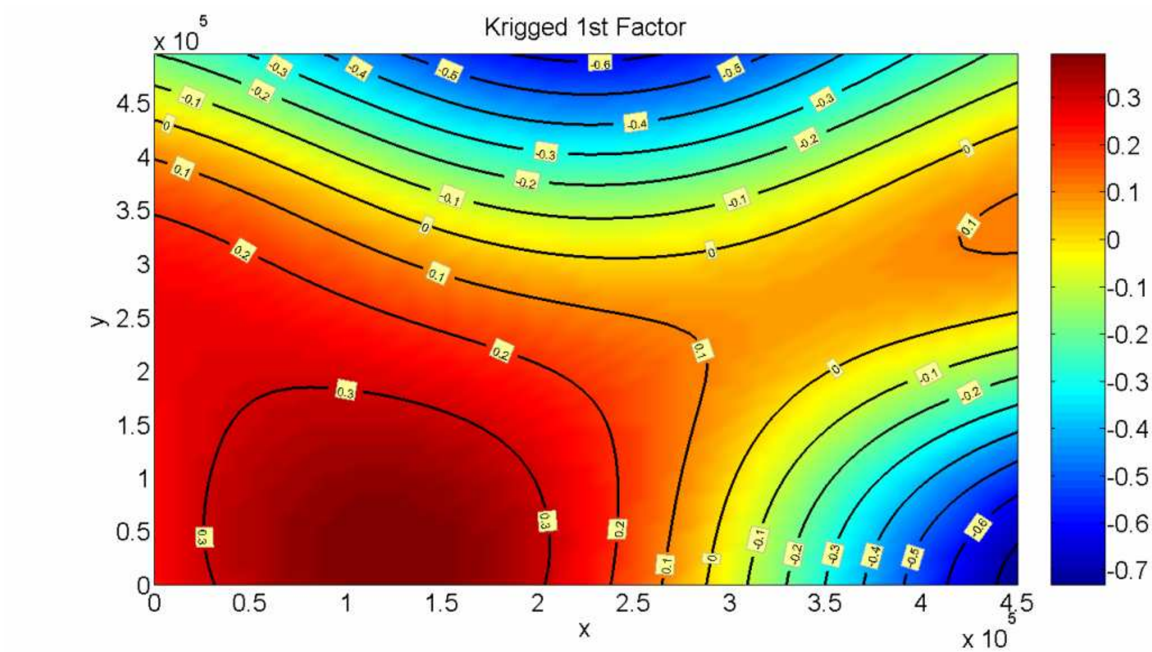

Figure 9. Spatial analysis of factor 1. (A) semi-variogram model; (B) kriging results.

(A)

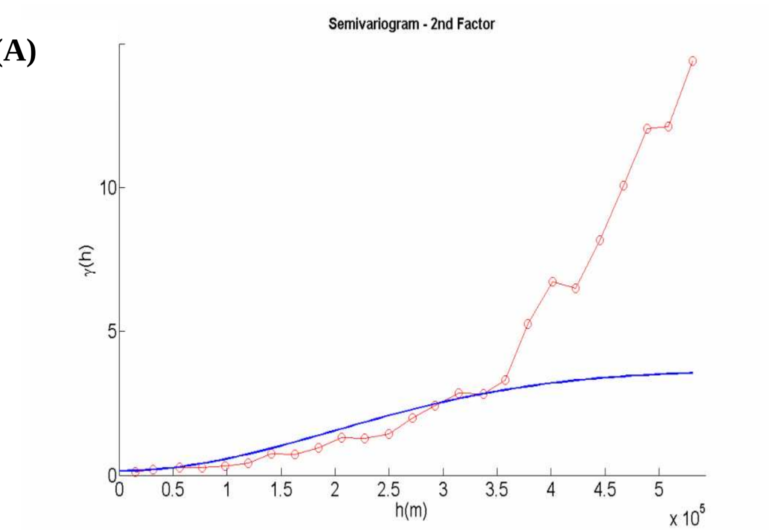

(B)

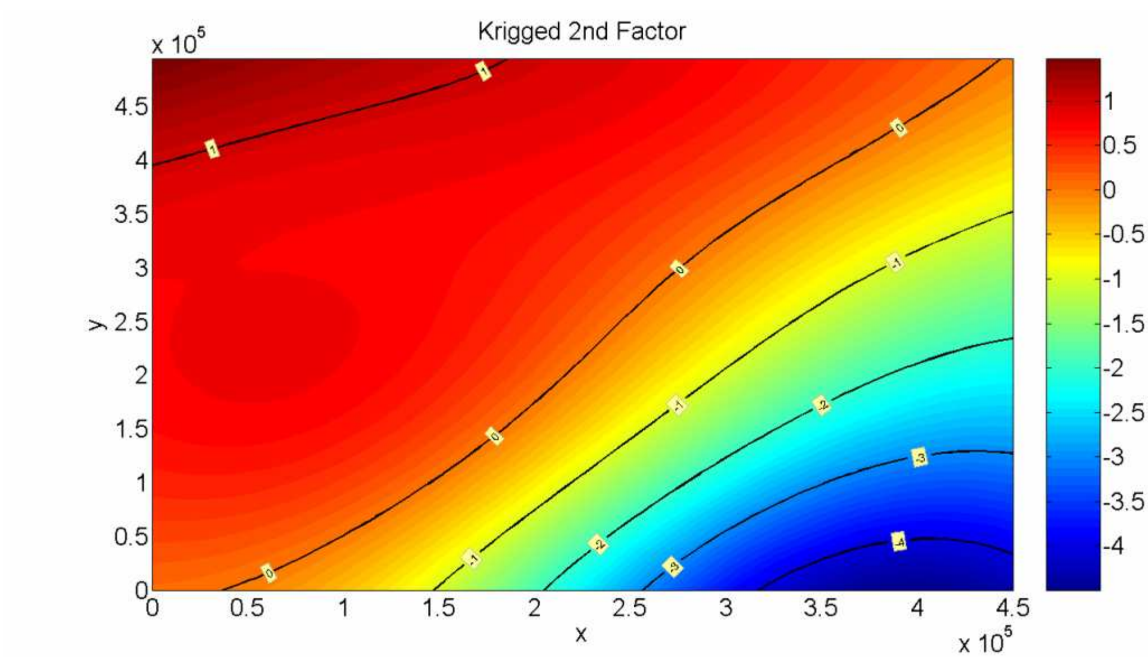

Figure 10. Spatial analysis of factor 2. (A) semi-variogram model; (B) kriging results.

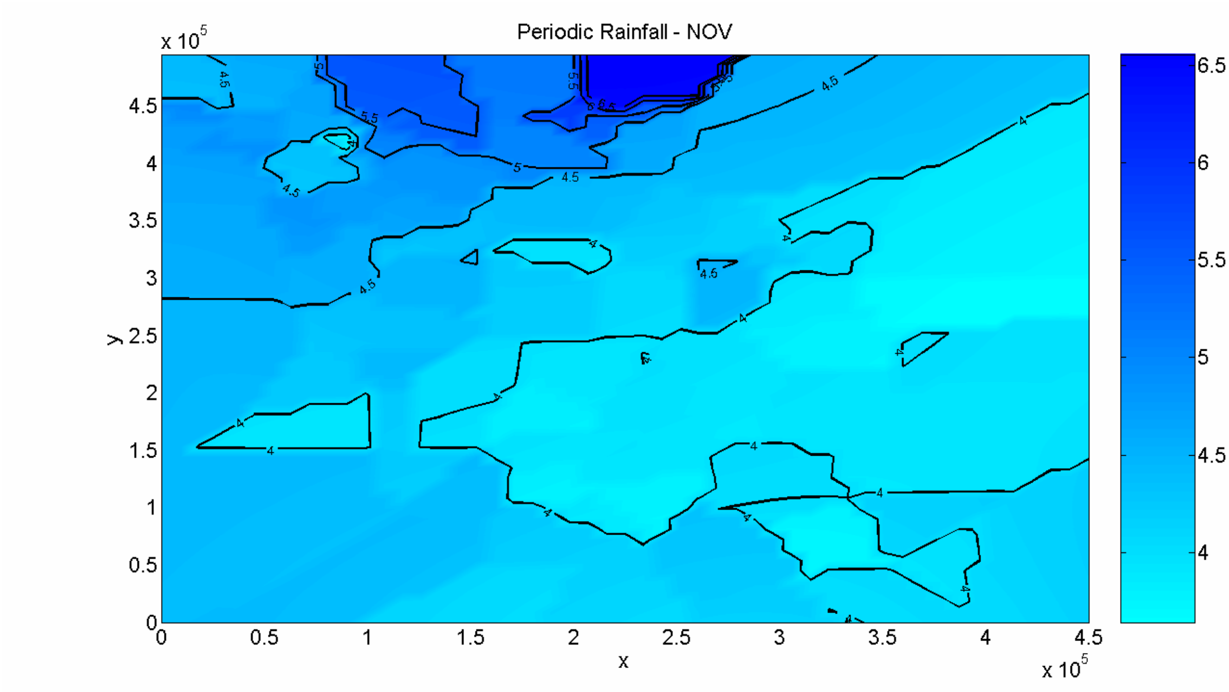

Figure 11. Generation of precipitation data of November by assuming independent Gaussian random fields of factors 1 and 2.

SPATIOTEMPORAL ANALYSIS OF GROUNDWATER WITHDWAL

The estimated 16,500 irrigation systems in Georgia use exclusively or a combination of groundwater, surface water and well to pond water as their water source. Georgia has identified various contributors to water withdrawals and withdrawal permitting schemes for agricultural purposes by issuing permits for withdrawal of water for industrial, municipal, or agricultural use for withdrawals that have the capacity to exceed 100,000 gallons per day (gpd) on a monthly average. As a result of the 1988 statues, many permitted water users were specifically exempted from water metering, record keeping, and reporting to EPD. In 1998, EPD requested that the Georgia Cooperative Extension Service (CES) establish a statewide system for measurement of water application by producers and conduct a multi-year study of those water amounts. From 1999-2004, a 2% random sample of irrigation systems and a 5% sample of ground-water-supplied systems was metered across Georgia. Flow rates on sampled irrigation systems were measured with “strap-on” digital flow meters, and usage hours were recorded monthly for each system. Additionally, crop type, wetted area, power source, and water source were determined during each observation.

Data

The Spring Creek Sub-basin of the Lower Flint River Basin hosts the highest density of agricultural users in the Flint River Basin of the Appalachicola watershed in Georgia. The Fall Line forms the southern boundary and separates North Georgia from the Coastal Plain (Figure 12B), where more than 95% of crop production and irrigation acreage lies. Agricultural water sources are typically 30% surface water and 70% groundwater south of the Fall Lin in Georgia. Approximately 250 mgd are used basin wide in the FRB by agricultural surface-water users in July (the peak month) of a typical irrigation season during a drought year, and approximately 950 mgd are withdrawn from Floridan aquifer irrigation wells at the peak of the irrigation season during a drought year (Couch et al, 2006).

The CES report contains annual average irrigation water withdrawals for each county in Georgia (see Appendex). North of the Fall Line in Georgia, few agricultural areas lie over high-yielding aquifers. South of the Fall Line, especially in Southwest Georgia, most farms are underlain by deep high-yielding aquifers, particularly the Floridan aquifer. Reliable withdrawals at rates exceeding 1000 gal/min are common with larger wells in those areas and as a result, southwestern Georgia has the highest density of groundwater use permits (Figure 13A). Furthermore, the more heavily irrigated areas fell within the Spring Creek Sub-basin. Statistical studies of stream discharge and biological studies of endangered fresh-water mussels indicate that Spring Creek sub-basin has exceeded its safe yield in terms of farm-use withdrawals (Couch et al, 2006). Using this information, the task of identifying counties for this study paper was straightforward. As a way to fully capture the impact that groundwater withdrawals have on groundwater levels, this paper focuses on counties in the Spring Creek Sub-basin which had the highest density of randomly selected irrigation systems (Figures 12A, 14): Baker, Calhoun, Decatur, Dougherty, Early, Lee, Miller, Mitchell and Worth.

For the purposes of statistical inferences, the irrigation water use random sampling strategy conducted by the CES group is assumed to have been identically, independently distributed. In the collection of the randomly sampled sites, each has the same probability distribution as the others and all are mutually independent. This assumption allows one to conclude that the proportion of sampled irrigation sites from county to county is an accurate reflection of the true irrigation system profile for the Lower Flint River Basin. Annual groundwater withdrawal amounts are elaborated in the Appendix.

Groundwater withdrawals used in my study are based on the weighted irrigation depths computed for each irrigation system by the CES group (see Appendix). This was accomplished by dividing annual total quantity or water pumped onto a field by the entire wetted area of that system, regardless of whether only a portion of that field was irrigation at that time. Statewide means for irrigation depth were calculated for each year for those individual systems. Unweighted averaged are averages of irrigation depths observed for each site. Weighted averages show the influence of wetted field size; weighting sums the volumes of water pumped in the stated and divides that by the sum of the wetted acres. The assumption was that the random stratified sampling achieved its purpose of proportionally sampling every type of field and use, and so the weighted average irrigation depth was the preferred value in calculations of total withdrawals as seen in Table 3.

(A) (B)

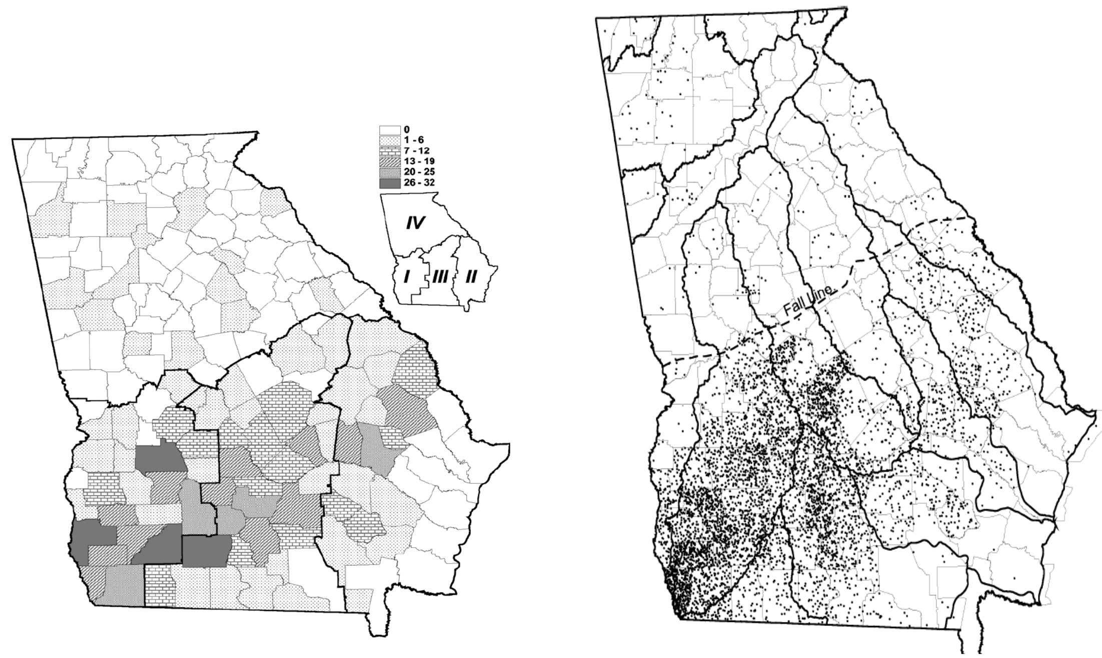

Figure 12. (A) Division of Goergia into four agricultural water permitting reportings regions and the number of sampling sites in each of Georgia counties from sampling in proportion to the number of permits issued in each county and (B) County by county irrigated area density (1 dot = 0.1% of irrigated field in 2000 overlying a map illustrating Georgia's 14 major drainage basins.

(A) **(B)**

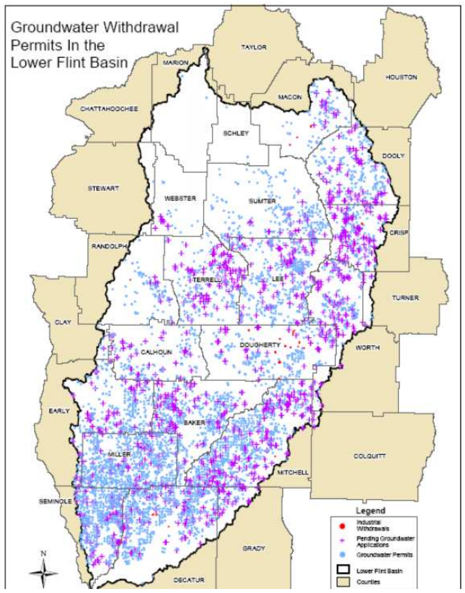

Figure 5.2: Pending and permitted ground-water locations

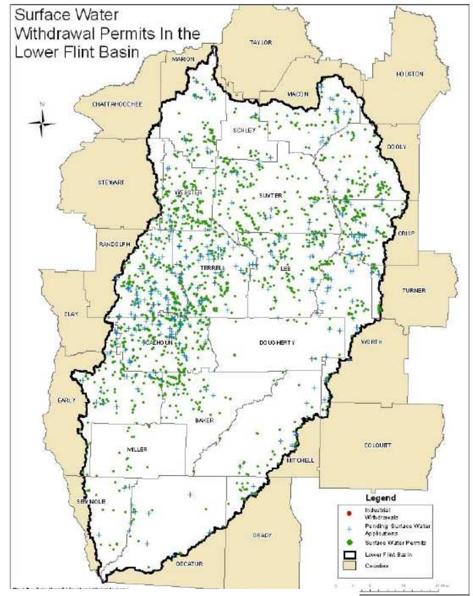

Figure 5.3. Pending and permitted surface-water withdrawal locations

Figure 13. Locations for pending and permitted groundwater withdrawal users in 2000 for Lower Flint River Basin in Georgia. and (b) Locations for pending and permitted surface water withdrawal users in 2000 for Lower Flint River Basin in Georgia.

Figure 14. Circle in the vicinity of Spring Creek sub-basin from which counties with highest number of randomly selected irrigation systems were selected.

The nine counties selected for this paper contained excellent examples of irrigation systems that used groundwater as their primary water source and there was a commendable collection of USGS gages with groundwater level records for the period 1999 through 2004.

In selecting appropriate USGS gages to accurately represent the characteristic hyrogeology of the Spring Creek Sub-basin, the Upper Floridan Aquifer exhibits a very close connection between the groundwater and surface water (Couch et al, 2006). In total, 17 USGS gages were selected to represent the Spring Creek Sub-basin (Table 4). The criteria for selecting a USGS gage in this paper are mainly driven by data availability. A particular county may have dozens of USGS gages but only a few have a period of record which overlaps that of the study period 2000-2004. The following was met in selecting the USGS gages to represent annual mean groundwater levels. Firstly, the gage must overly the Floridan Aquifer; secondly the gage must reflect monthly groundwater level measurements as best as possible for years 1999 - 2004.

The USGS gage locations were given in latitude and longitude and had to be converted into a different set of units that would resemble the spatial distance in between gages. The conversion was simply done assuming that the Earth is a sphere but that the distances between gages are small enough that the ground can be considered flat. Figure 15 shows a spatial representation of USGS groundwater observation sites withing upper Floridan Aquifer in Southwest Georgia in distance, feet.

Table 3. Mean annual are-weighted irrigation depths and calculated withdrawals by county and water source for 2002 in the Southwest region. For means calculated from less than 5 samples (indicated by *) from within the county and its adjacent neighboring counties, withdrawals were calculated from region-wide means for that source [Hook et al, 2005].

County	GW	SW	W2P	GW	SW	W2P	All	County-wide Irr Depth
	------------ in./yr ------------			-------------------- Mgal/yr -------------------				in./y
Baker	10.5	8.1	9.2	13,300	790	670	14,800	2.4
Calhoun	10.5	6.8	8.2	6,500	2,300	980	9,800	1.98
Chattahoochee	10.0*	7.3*	7.7*	0	0	0	0	0.000
Clay	8.7	6.0	8.2	330	1,110	160	1,600	0.42
Crawford	10.0*	7.3*	7.7*	700	116	0	820	0.145
Crisp	8.5	7.6	7.9	3,900	580	370	4,900	0.99
Decatur	11.8	8.2	12.9	28,000	2,700	210	31,000	2.9
Dooly	7.00	6.8	6.0	5,200	320	610	6,100	0.88
Dougherty	10.8	10.0	7.8	5,800	400	310	6,500	1.11
Early	9.2	8.9	8.2	9,000	2,300	3,200	14,500	1.61
Lee	10.3	8.3	8.2	11,600	460	720	12,800	2.0
Macon	6.2	5.8	5.3	3,100	930	210	4,200	0.60
Marion	7.8	4.8	7.7	84	230	37	350	0.055
Miller	10.0	9.0	9.3	11,900	1,030	1,740	14,700	3.0
Mitchell	13.1	7.6	8.3	25,000	3,90	580	29,000	3.3
Muscogee	10.0*	7.3*	7.7*	0	250	0	250	0.068
Quitman	10.0*	3.3	7.7*	0	23	0	23	0.008
Randolph	8.1	5.4	7.7*	2,300	1,760	1,310	5,300	0.70
Schley	6.6	5.3	4.3	63	150	0	210	0.079
Seminole	9.7	9.2	9.3	12,500	1,290	1,190	15,000	3.4
Stewart	10.0*	2.7	7.7*	0	210	0	210	0.026
Sumter	8.0	8.5	5.3	4,800	4,800	530	10,100	1.20
Taylor	10.0	4.8	7.7*	1,900	650	360	2,900	0.50
Terrell	10.0	7.7	10.8	3,300	2,900	500	6,700	1.14
Webster	7.7	5.2	7.7*	120	870	20	1,000	0.28
Worth	11.0	8.6	6.8	8,200	3,200	1,300	12,700	1.28
Southwest GA	10.0	7.3	7.7	157,000	34,000	14,600	210,000	

Table 4. USGS Gages overlying the Upper Floridan Aquifer in Spring Creek Sub-basin of Georgia.

County	USGS Gage Identification Number	Latitude	Longitude	Number of Observations [1999 2000 2001 2002 2003 2004]	Observation Interval (Convential Dates)	
Baker_A	312617084110701	31.43825	84.18502778	[11 11 5 4 6 2]	2/5/1999	9/2/2004
Baker_B	311400084295502	31.23333333	84.49861111	[12 11 10 10 10 9]	1/14/1999	11/10/2004
Calhoun	312853084275101	31.48138889	84.46416667	[11 11 10 10 9 6]	2/8/1999	10/15/2004
Decatur_A	310428084310501	31.07444444	84.51805556	[12 10 12 7 9 7]	1/13/1999	11/11/2004
Decatur_B	305736084355801	30.96166667	84.59611111	[13 13 6 6 4 4]	1/13/1999	9/29/2004
Dougherty_A	312950084131801	31.49758333	84.22152778	[12 10 10 10 11 6]	1/15/1999	10/20/2004
Dougherty_B	313450084091801	31.58055556	84.155	[12 10 10 10 10 7]	1/19/1999	10/25/2004
Dougherty_C	313040084125901	31.51161111	84.20919444	[12 10 12 12 10 10 6]	1/15/1999	11/15/2004
Dougherty_D	313019084104601	31.50538889	84.17952778	[- 7 12 10 12 11]	7/10/2000	11/1/2004
Dougherty_E	313521084051001	31.58916667	84.08611111	[12 10 10 10 9 7]	1/14/1999	11/30/2004
Early	312232084391701	31.37722222	84.65472222	[12 14 8 4 4 3]	1/12/1999	9/8/2004
Lee	313808084093601	31.63555556	84.16	[16 12 6 3 4 3]	1/14/1999	9/9/2004
Miller_A	310651084404501	31.11416667	84.67888889	[12 15 8 6 5 5]	1/13/1999	8/17/2000
Miller_B	311009084495502	31.16888889	84.83166667	[11 11 10 11 10 7]	2/11/1999	11/10/2004
Mitchell_A	311802084192302	31.30055556	84.32305556	[13 12 10 10 10 7]	1/13/1999	11/11/2004
Mitchell_B	312127084065801	31.35805556	84.11583333	[13 13 8 5 4 3]	1/14/1999	8/9/2004
Worth	314330084005402	31.725	84.01416667	[13 11 11 11 11 12]	1/7/1999	11/30/2004

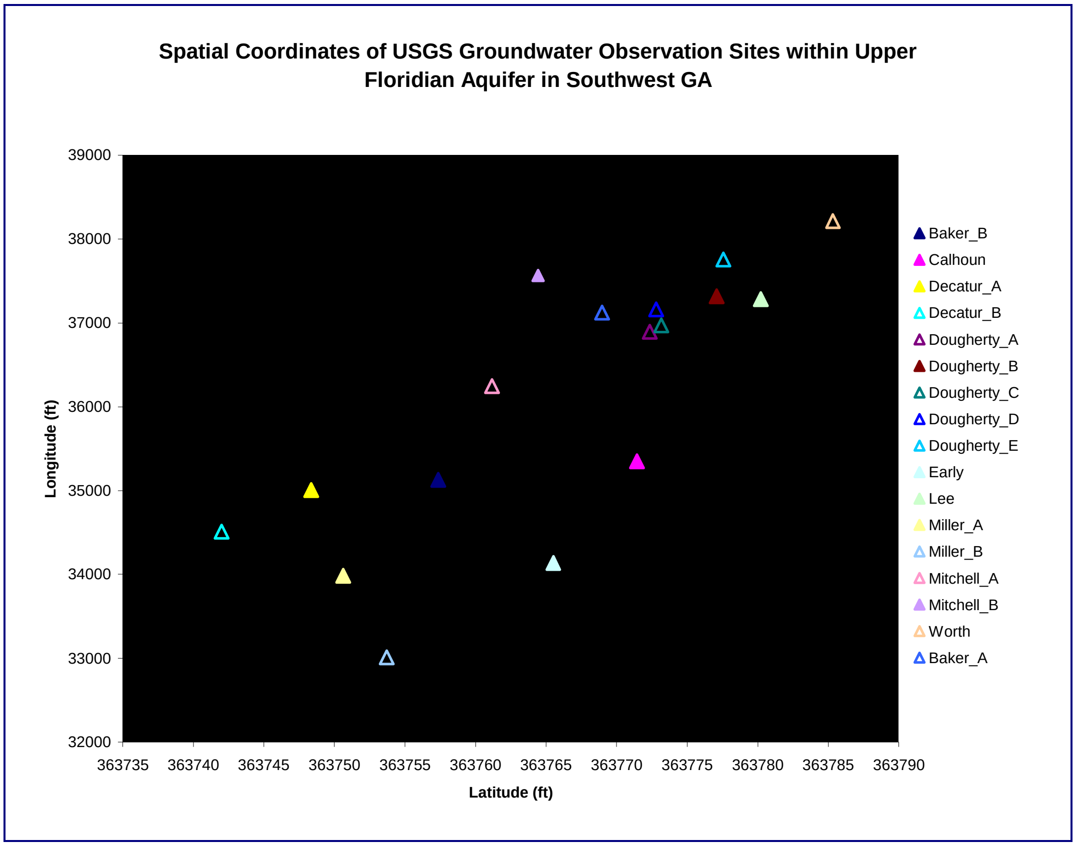

Figure 15. Spatial representation of USGS groundwater observation sites withing upper Floridan Aquifer in Southwest Georgia in distance, feet.

Semi-variograms

Both spatial and temporal experimental variograms were constructed using the groundwater level data available at the 17 USGS gages in the study area. The spatial distribution of gage sites shown in Figure 4 is thought to hold much potential in producing a two dimensional profile groundwater levels for an area with dimensions 43.32 by 5203.23 feet. Within the confines of these dimensions are the 9 counties selected for the spatial analysis. Groundwater levels at the gage sites are pre-processed by computing mean annual values based on the available number of observations each year. Note that the distance scale for the spatial variogram reflects latitude and longitude due to computational constraints encountered when trying to use English units of distance (feet). Odd numbered Figures 17 – 25 display the final experimental variogram fit chosen after successive attempts to improve validation statistics and the corresponding predition model using ordinary kriging.

The temporal data used to construct experimental variograms for groundwater levels came from the year and date on which the measurement was taken at the USGS site and was transformed into a date series, much in the same way Julian days are calculated. It was thought that for each county, a one dimensional temporal experimental variogram could be constructed to characterize the temporal continuity or roughness of the data set. The groundwater level prediction model took form using ordinary kriging and the prediction interval varied by county but consistently spanned the years 2000 through 2004. In constructing the temporal groundwater level prediction models using the experimental variogram, the quantity and frequency of available data played a key role in minimizing the 95% confidence intervals. This is discussed further in the results section. Figures 26 – 28 display the final selection for the experimental temporal variogram model for selected counties with interesting characteristic groundwater prediction models.

Experimental spatial variograms were constructed in an attempt to determine the distribution of groundwater withdrawals for the study area. Since the exact preprocessing procedure used to compute the weighted annual average groundwater withdrawals for each county is not readily available, the assumption was made that the weighted mean value could be used for any spatial location within a given county. This meant that in cases were there was more than one spatial location in a county, the mean value of groundwater withdrawal held constant for those locations. The final selection of experimental variogram model and groundwater withdrawal prediction model are in even numbered Figures 16 – 24.

This inconvenience led to the exploration of how one might go about developing an experimental model that described the correlative characteristics or interdependence between groundwater level and groundwater withdrawal. Would it be possible to estimate the cross-covariance between these two variables in order to predict one knowing only about the other? The question begs an answer, but before going further on this topic, it is important to explore the possibility that I may have found a qualifying dataset for such an interesting analysis.

In all the variogram model analyses conducted in this study, the greatest effort was placed on obtaining an experimental variogram that accurately representing the observed data near the origin. The best validation statistics were obtained with an exponential model in each of the three cases mentioned, (1) Spatial variograms for annual groundwater levels for years 2000-20004(2) Spatial variogram for annual groundwater withdrawals for year 2000 -2004 and (3) Temporal variogram for groundwater levels at each county.

Validation statistics and summary of all experimental variogram model selection parameters are in Tables 5 – 7 for the spatial and temporal variogram analyses.

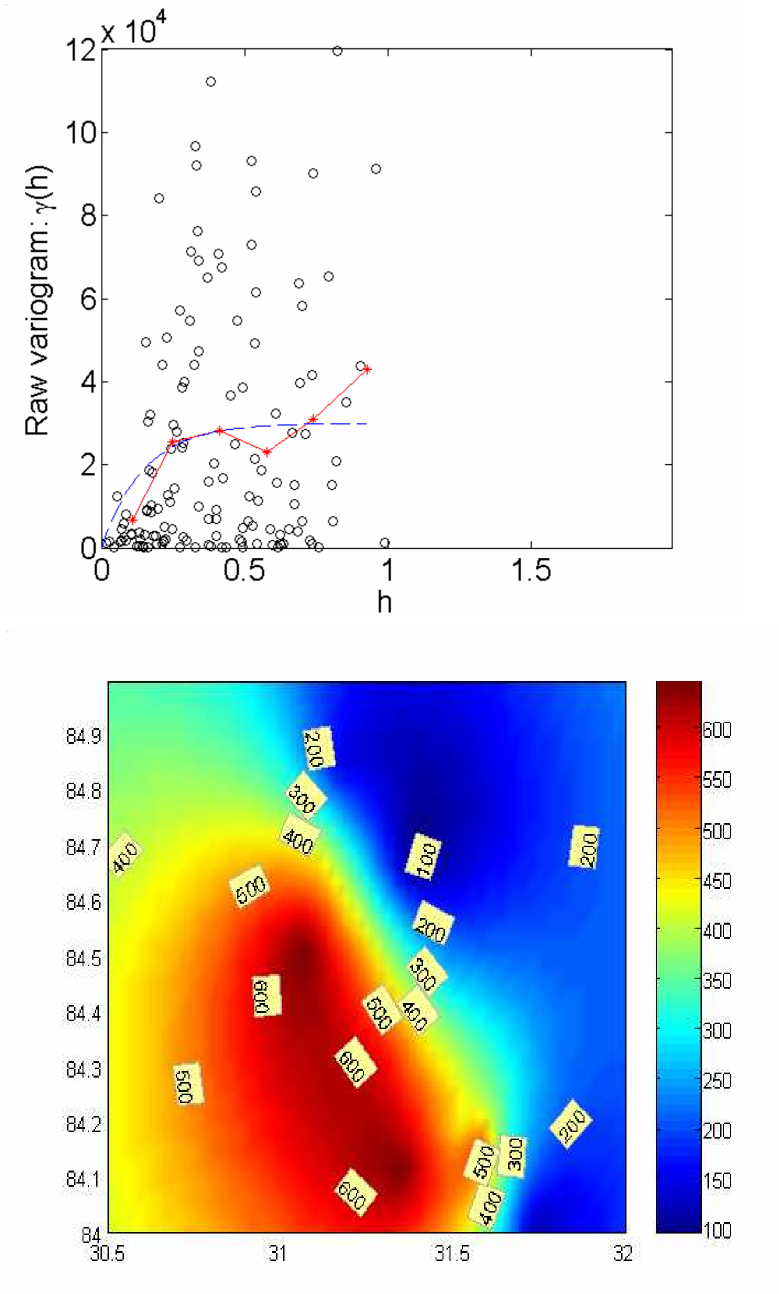

Figure 16. (A) Spatial Variogram and (B) Prediction Model for Groundwater levels in 2000.

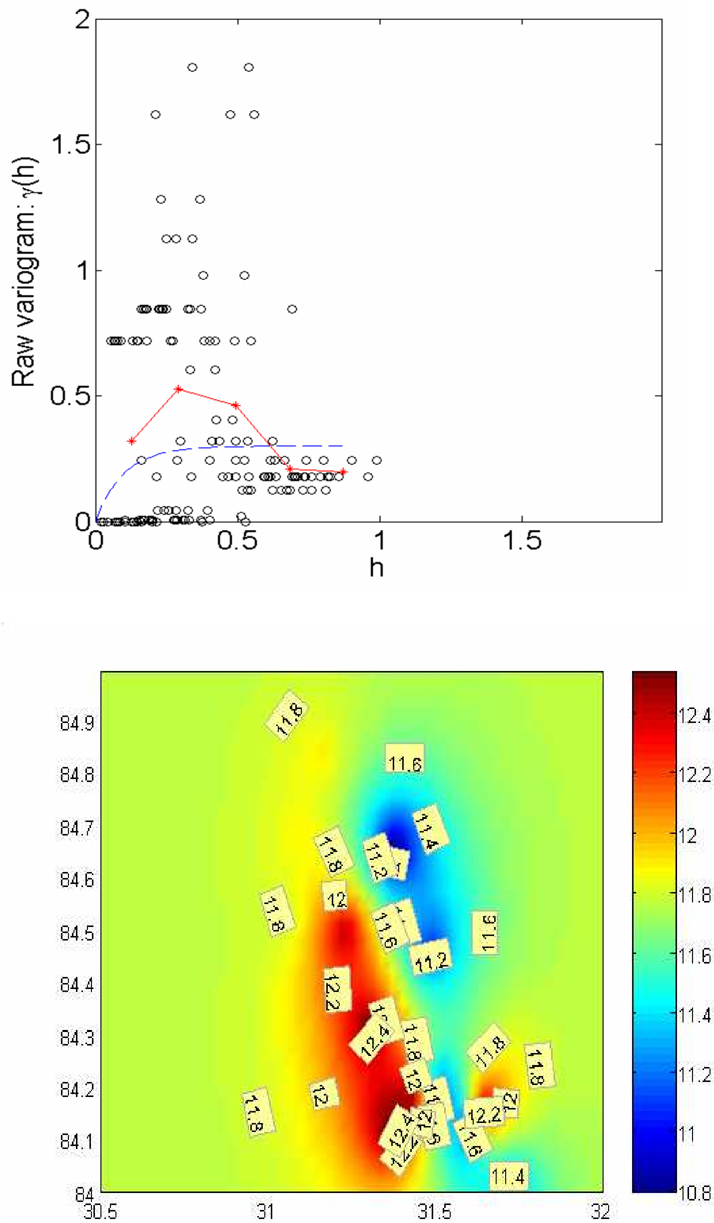

Figure 17. Spatial Variogram (A) and Prediction Model (B) for Groundwater Withdrawal Quantities 2000.

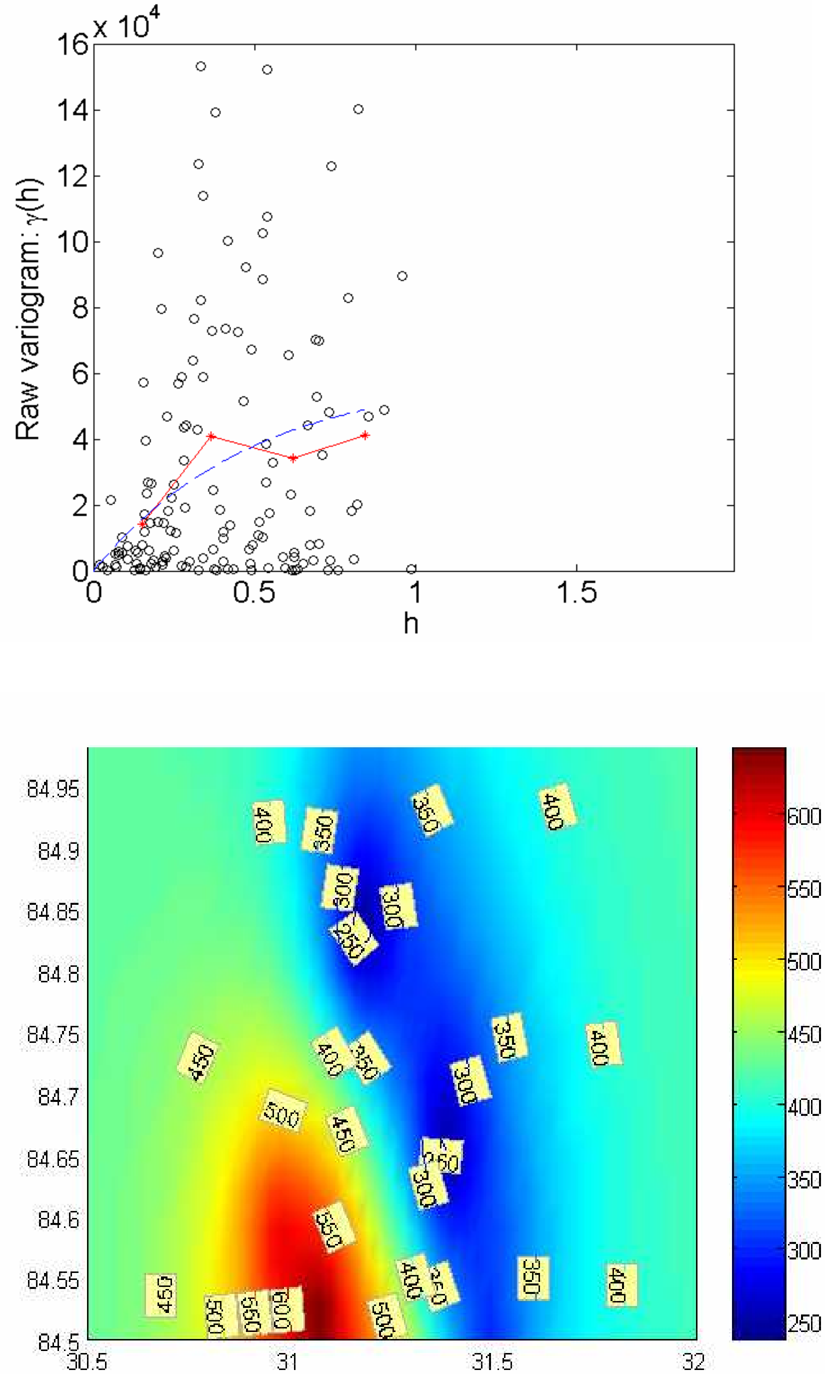

Figure 18. (A) Spatial Variogram and (B) Prediction Model for Groundwater levels in 2001.

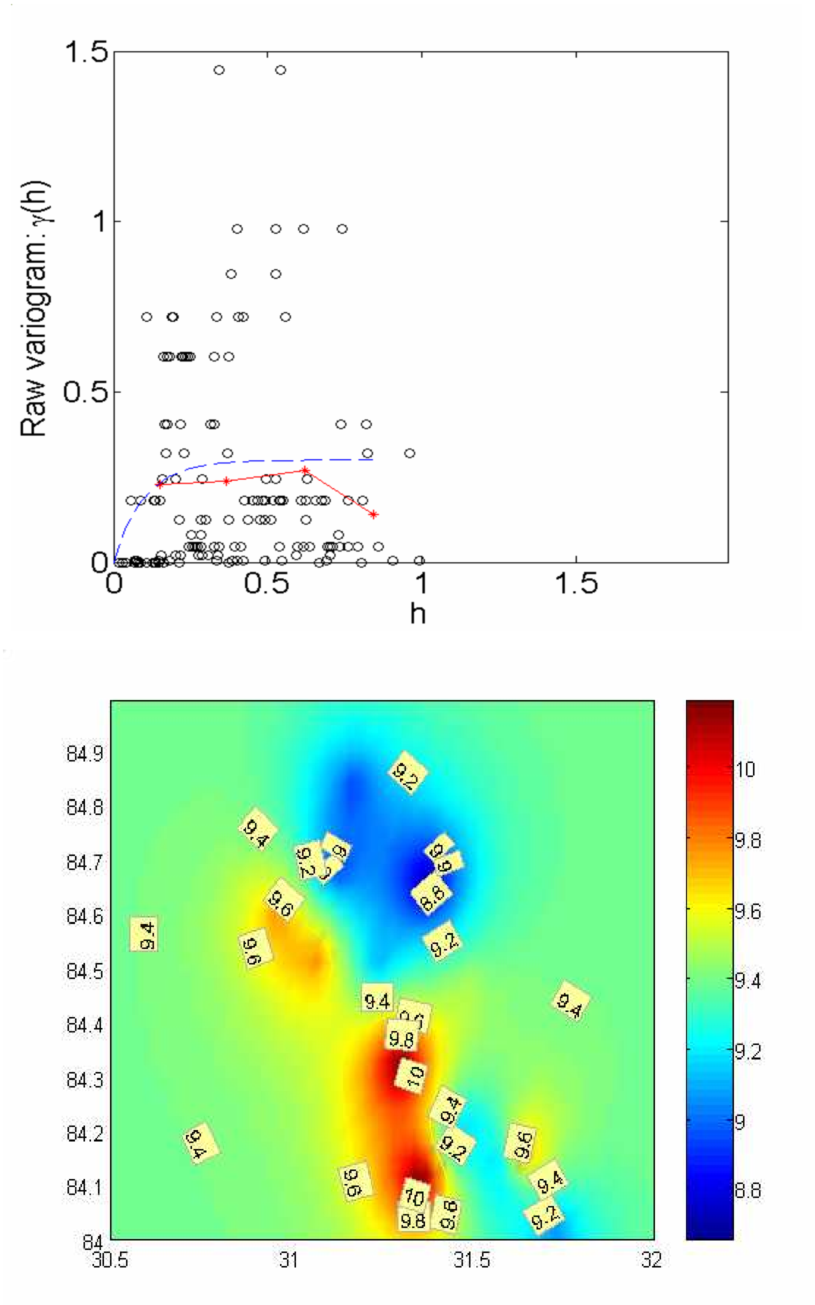

Figure 19. Spatial Variogram(A) and Prediction Model (B) for Groundwater Withdrawal Quantities 2001.

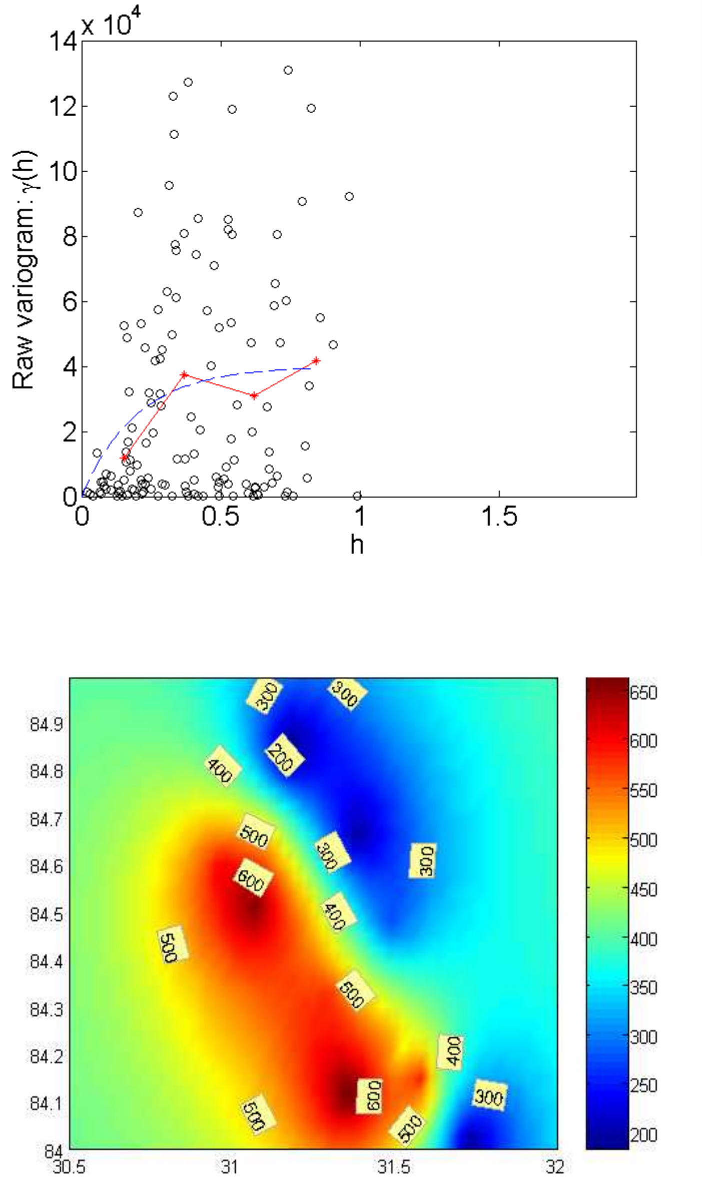

Figure 20. (a) Spatial Variogram and (b) Prediction Model for Groundwater levels in 2002.

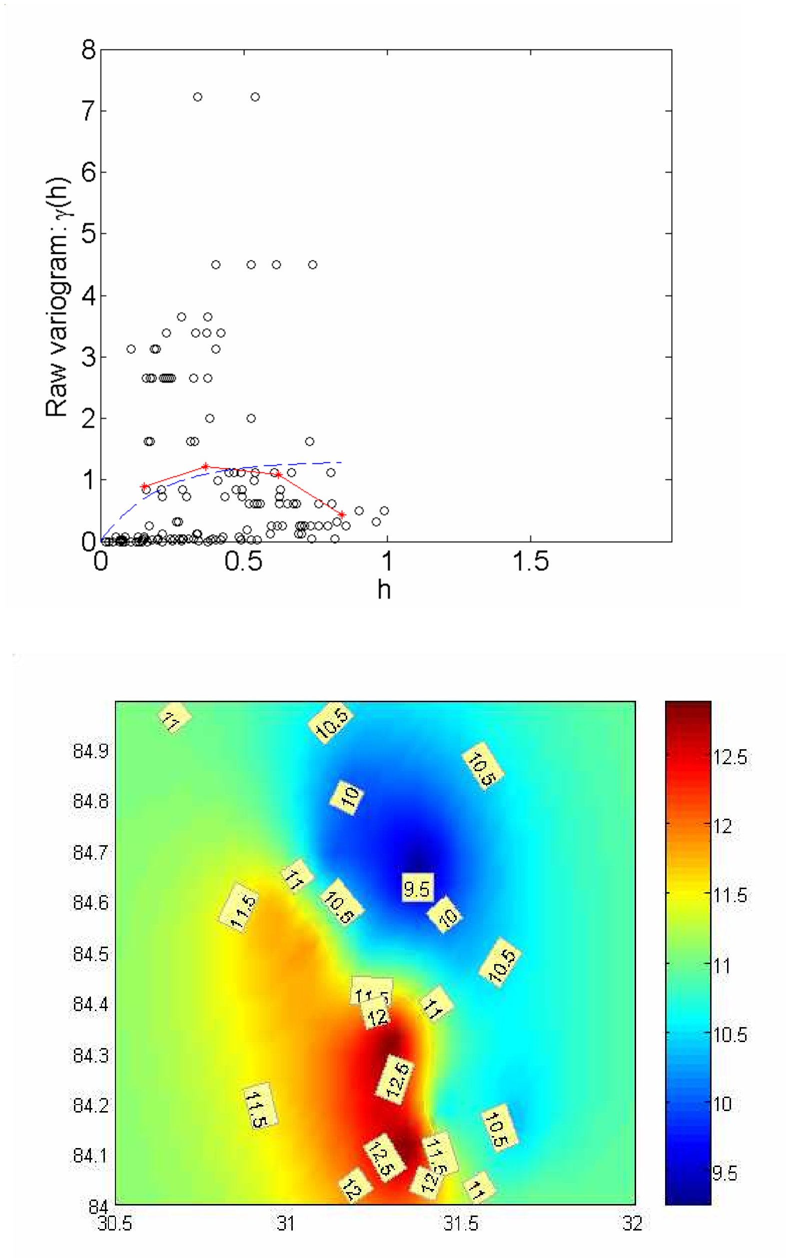

Figure 21. Spatial Variogram (a) and Prediction Model (b) for Groundwater Withdrawal Quantities 2002.

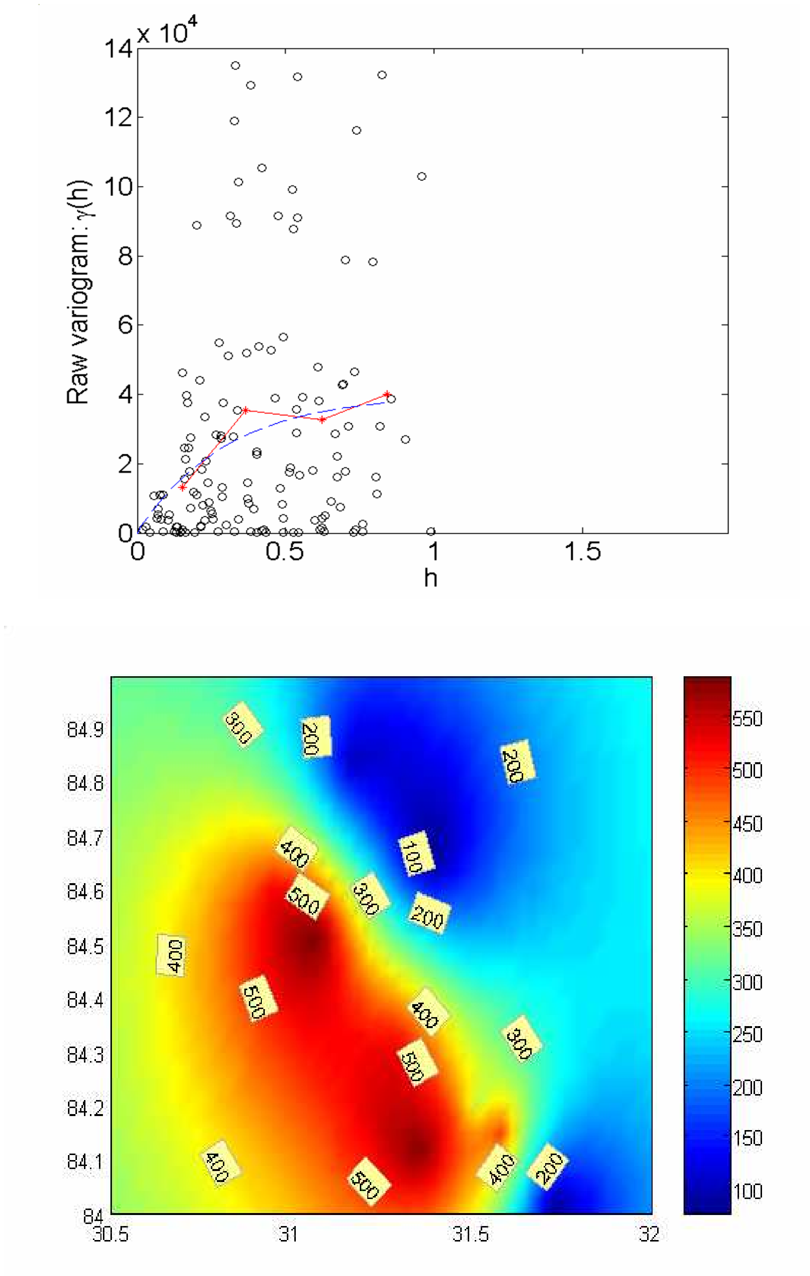

Figure 22. (a) Spatial Variogram and (b) Prediction Model for Groundwater levels in 2003.

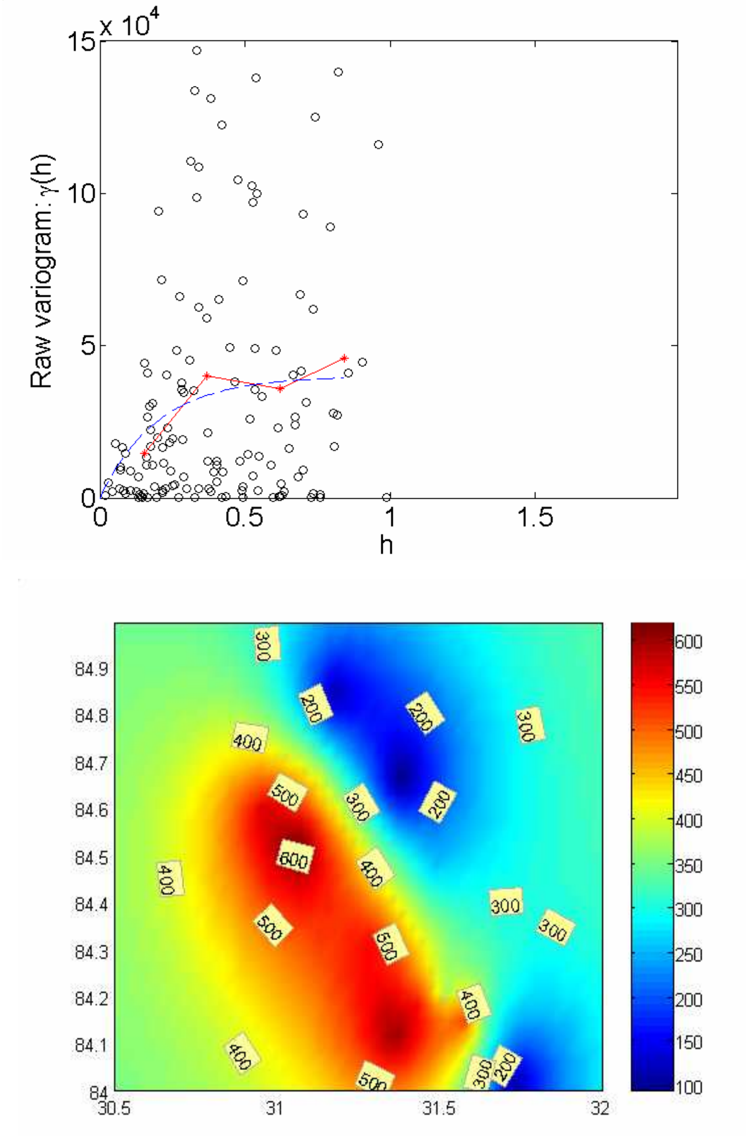

Figure 23. Spatial Variogram (a) and Prediction Model (b) for Groundwater Withdrawal Quantities 2003.

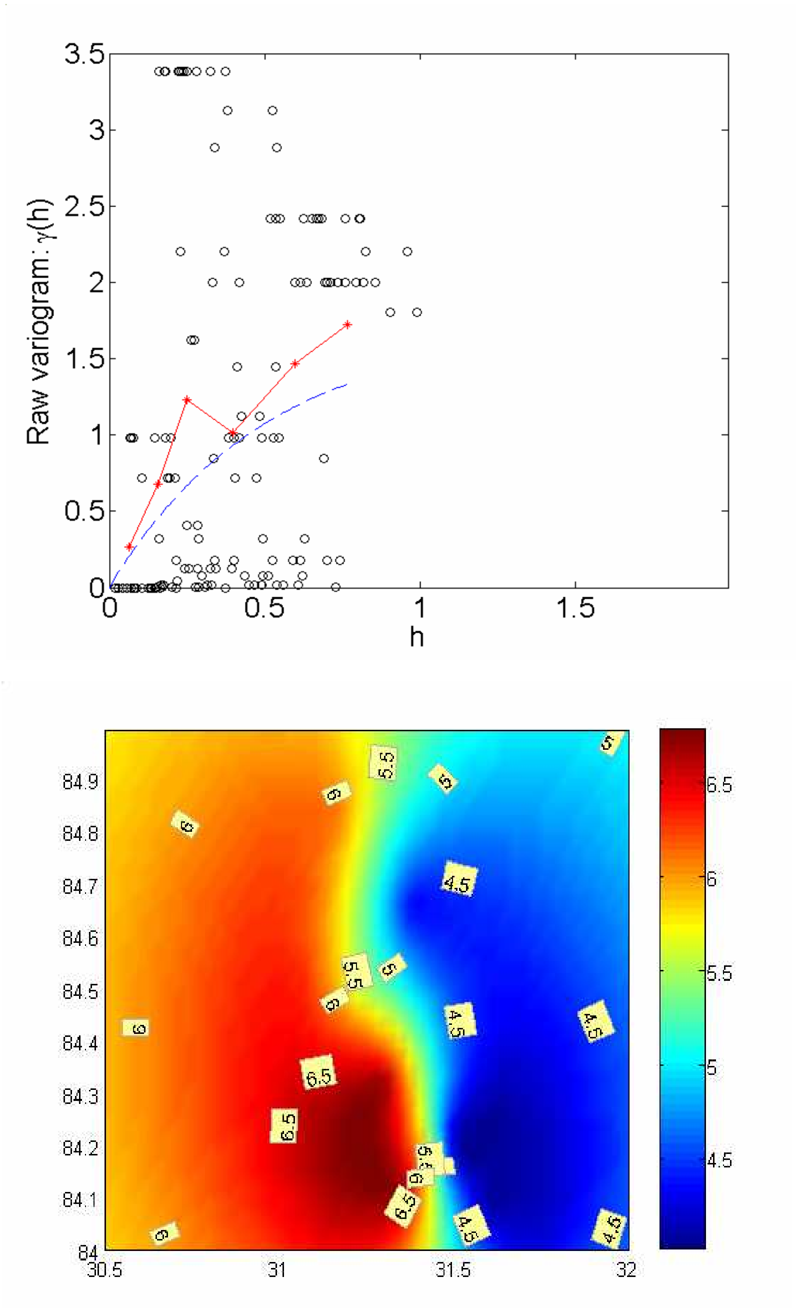

Figure 24. Spatial Variogram (a) and Prediction Model (b) for Groundwater Withdrawal Quantities 2004.

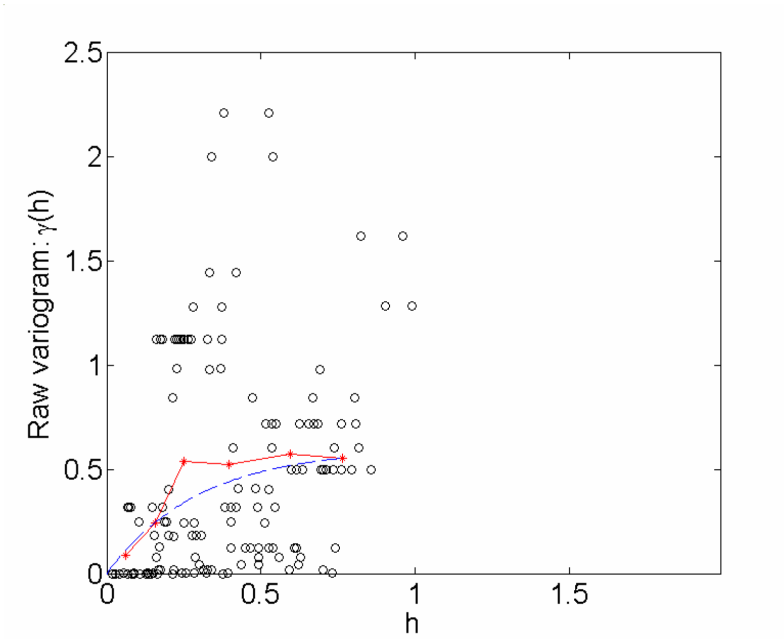

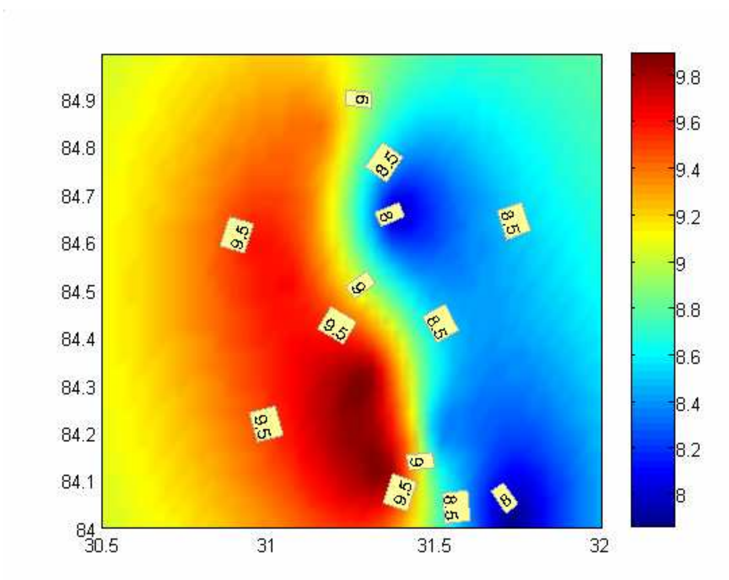

Figure 25. Spatial Variogram (a) and Prediction Model (b) for Groundwater Withdrawal Quantities 2004.

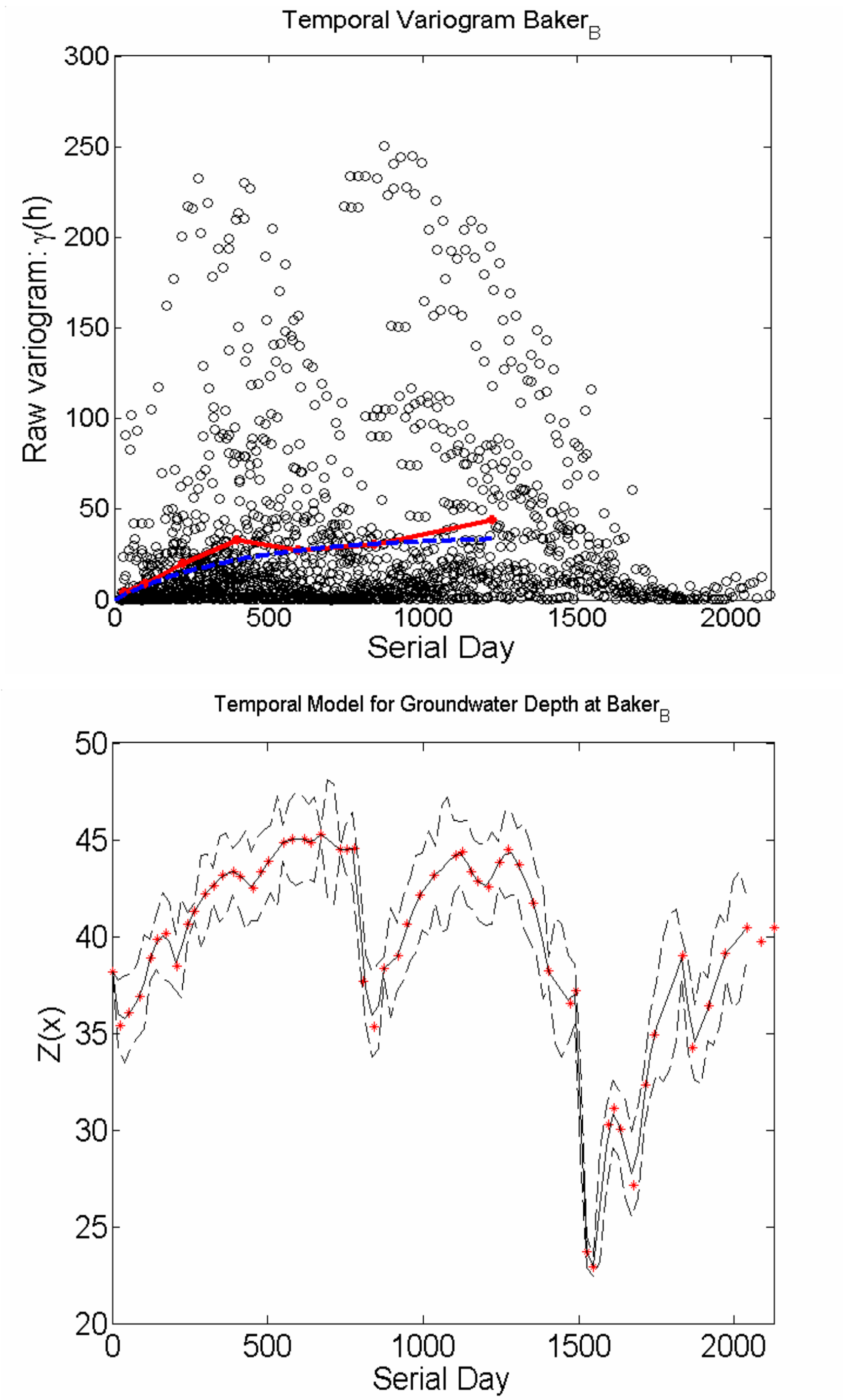

Figure 26. Temporal Variogram (a) and Prediction Model (b) for Groundwater level at Baker$_B$ for the observation period 2/5/1999 – 9/2/2004.

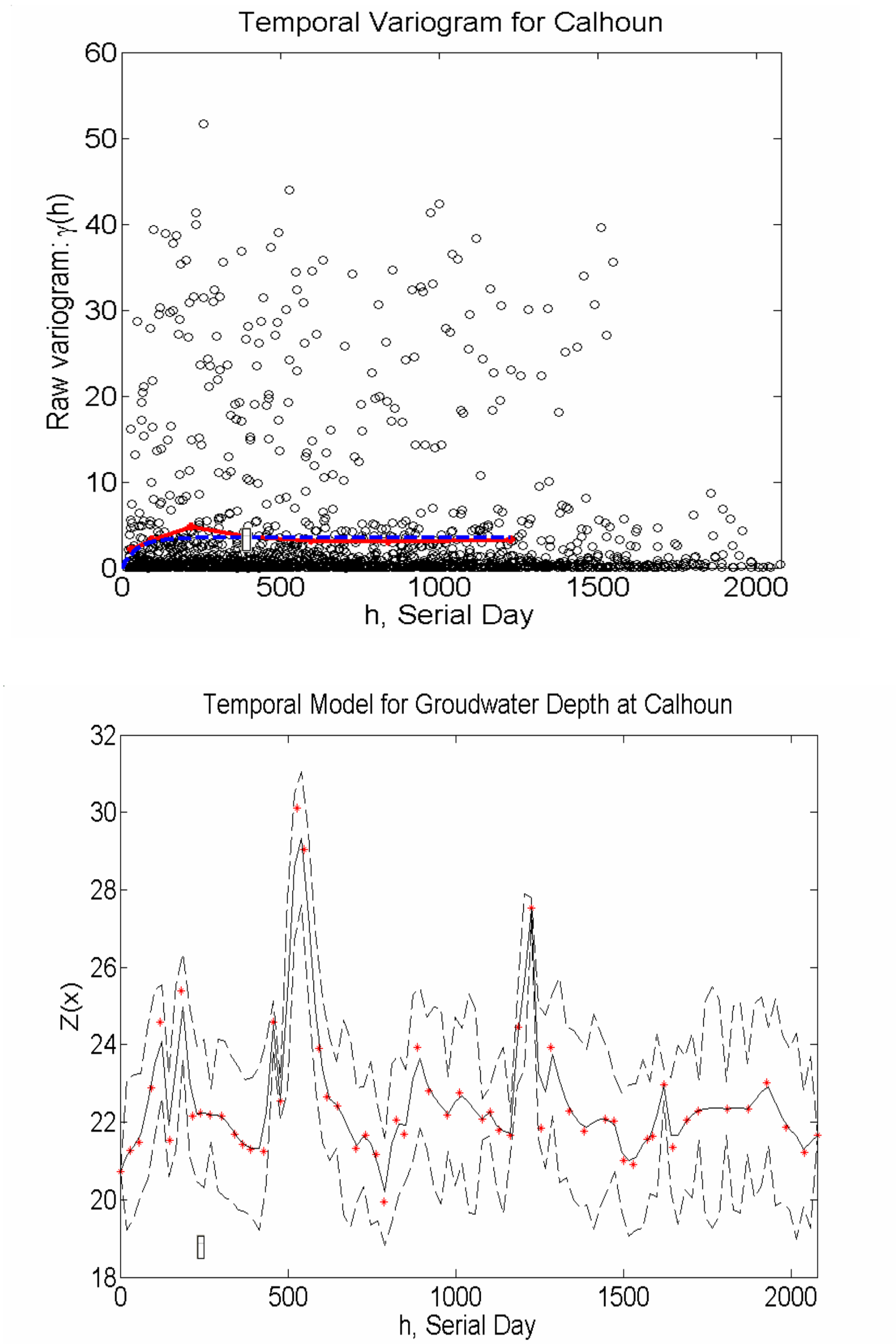

Figure 27. Temporal Variogram (a) and Prediction Model (b) for Groundwater level at Calhoun for the observation period 1/14/1999 – 11/10/2004.

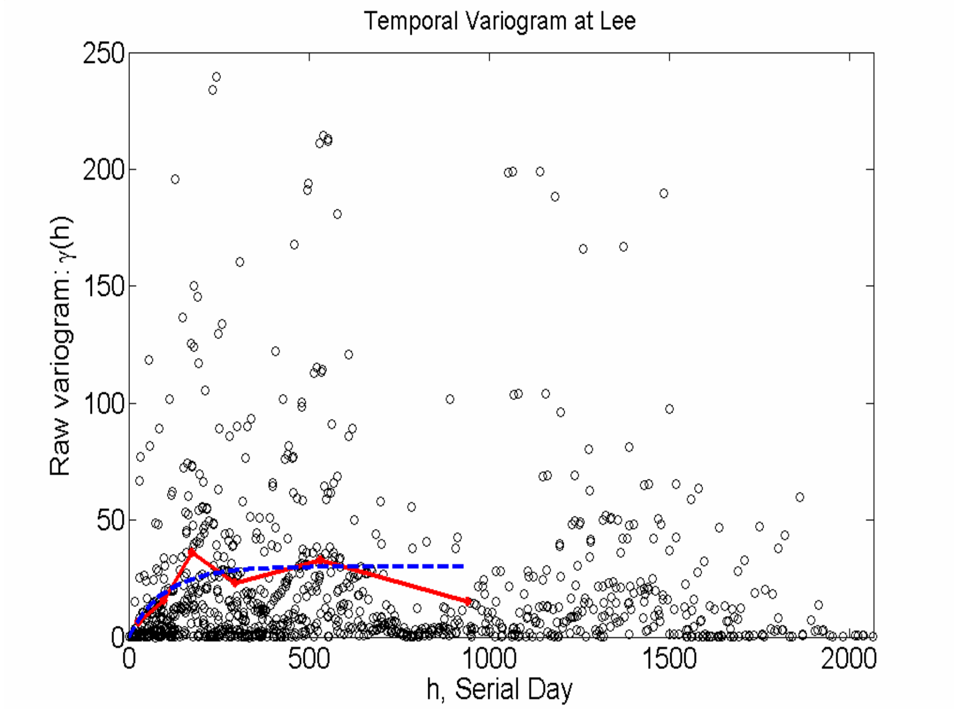

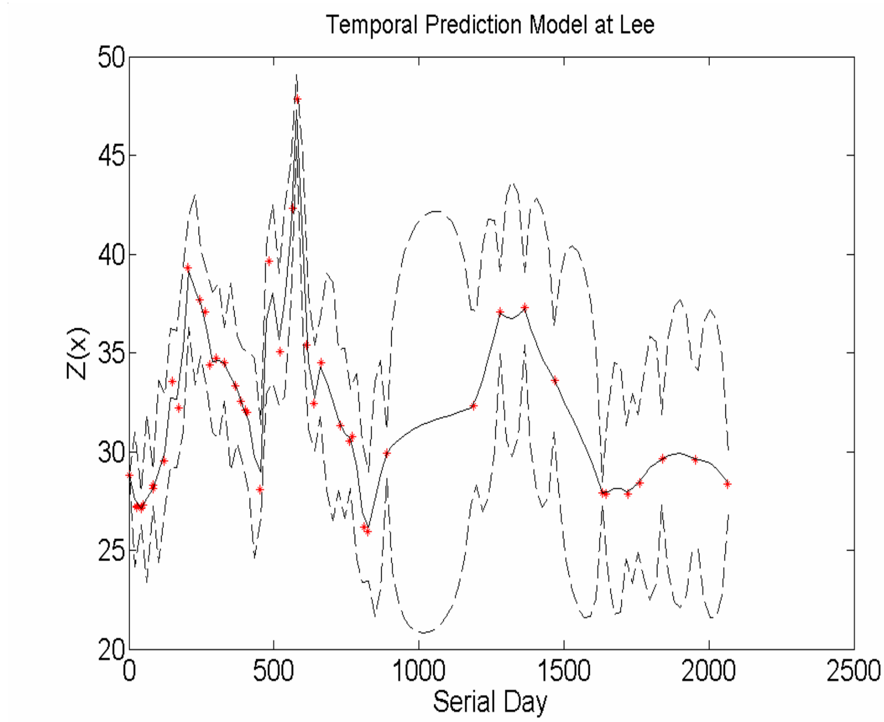

Figure 28. Temporal Variogram (a) and Prediction Model (b) for Groundwater level at Lee for the observation period 1/12/1999 – 9/8/2004.

Table 5. Summary statistics for spatial exponential variograms of Groundwater levels study area of Georgia for years 2000 – 2004.

Exponential Variogram Model Validation					
Annual Average Depth to Groundwater in SW Irrigation Counties in GA					
Year	Variance	Length	Q1	Q2	cR
2000	30000	0.15	-0.3359	0.79731	21483.0695
2001	60000	0.5	-0.4587	0.95724	18166.6059
2002	40000	0.2	-0.3477	0.75251	24243.0773
2003	40000	0.3	-0.4486	0.92399	18299.7846
2004	40000	0.2	-0.4214	0.87071	24243.0773

Table 6. Summary statistics for spatial exponential variograms of Groundwater withdrawals in study area of Georgia for years 2000 – 2004.

Exponential Variogram Model Validation					
Annual Average Depth to Groundwater in SW Irrigation Counties in GA					
	Variance	Length	Q1	Q2	cR
2000	0.3	0.1	-0.2627	1.5354	0.25786
2001	0.3	0.1	0.19215	0.89035	0.25786
2002	1.3	0.2	0.21659	1.002	0.7879
2003	1.7	0.5	-0.0455	0.84191	0.51472
2004	0.6	0.3	-0.1536	0.82687	0.2745

Table 7. Summary statistics for temporal exponential variograms for groundwater levels during study period at selected counties within study area in Georgia.

Georgia County	Validation Statistics			Exponential Model Parameters		Interval	Prediction Interval (Serial Value)		Prediction Interval (Convential Date)	
	Q1	**Q2**	**cR**	**Var**	**Length**	**Non-Uniform**	**tmin**	**tmax**	**tmin**	**tmax**
Lee	0.314	0.807	12.257	30	100	[50 150 200 400 700 1200]	0	2066	1/12/1999	9/8/2004
Baker_B	-0.029	1.266	5.447	35	400	[50 150 300 500 700 1000 1500]	0	2026	2/5/1999	9/2/2004
Calhoun	0.012	1.044	2.658	3.5	50	[50 150 300 500 700 1000 1500]	0	2127	1/14/1999	11/10/2004

Covariance Analysis

The usefulness of the data selected for this paper becomes evident when covariance calculations are made (Table 8). In this analysis, three parameters are considered: Mean annual irrigation depth by year and county, mean annual groundwater level by depth and county and mean annual groundwater withdrawals by year and county. Of the agricultural use data available for analysis in this paper, mean annual irrigation depth and mean annual groundwater withdrawal amounts are pre-processed values as described earlier in the text. However, based on the information known about irrigation water use in the study area, the dependency of groundwater withdrawals and irrigation depths is expected to be high. This is because the characteristic irrigation profile of the Spring Creek Sub-basin is one in which irrigation water sources are 30% surface and dominated by 70% groundwater. Additionally, the covariance statistic for these two variables is expected to perform well because of greater data availability in the CES study.

The measure of dependency between groundwater levels and withdrawals is of great interest and importance in determining how irrigation schemes affect the hydrology of a region. The outcome of this analysis is discussed in the results section.

Table 8 (a-e). Covariance calculations in test for correlations between mean irrigation depth, groundwater level and groundwater withdrawals for all counties, separated by year.

2000 Covariance Matrix for Upper Floridian Aquifer in SW GA			
	Mean Annual Irrigation Depth (in)	Mean Annual GW Withdrawal (in)	Mean Annual Depth to Groundwater (in)
Mean Annual Irrigation Depth (in)	0.81	0.38	24.60
Mean Annual GW Withdrawal (in)	0.38	0.36	46.43
Mean Annual Depth to Groundwater (in)	24.60	46.43	21948.40

(a)

2001 Covariance Matrix for Upper Floridian Aquifer in SW GA			
	Mean Annual Irrigation Depth (in)	Mean Annual GW Withdrawal (in)	Mean Annual Depth to Groundwater (in)
Mean Annual Irrigation Depth (in)	0.48	0.14	24.87
Mean Annual GW Withdrawal (in)	0.14	0.22	49.57
Mean Annual Depth to Groundwater (in)	24.87	49.57	28263.26

(b)

2002 Covariance Matrix for Upper Floridian Aquifer in SW GA			
	Mean Annual Irrigation Depth (in)	Mean Annual GW Withdrawal (in)	Mean Annual Depth to Groundwater (in)
Mean Annual Irrigation Depth (in)	0.69	0.38	33.79
Mean Annual GW Withdrawal (in)	0.38	0.95	98.99
Mean Annual Depth to Groundwater (in)	33.79	98.99	25861.11

(c)

2003 Covariance Matrix for Upper Floridian Aquifer in SW GA			
	Mean Annual Irrigation Depth (in)	Mean Annual GW Withdrawal (in)	Mean Annual Depth to Groundwater (in)
Mean Annual Irrigation Depth (in)	0.30	0.54	20.89
Mean Annual GW Withdrawal (in)	0.54	1.06	68.17
Mean Annual Depth to Groundwater (in)	20.89	68.17	25987.92

(d)

2004 Covariance Matrix for Upper Floridian Aquifer in SW GA			
	Mean Annual Irrigation Depth (in)	Mean Annual GW Withdrawal (in)	Mean Annual Depth to Groundwater (in)
Mean Annual Irrigation Depth (in)	0.53	0.43	36.65
Mean Annual GW Withdrawal (in)	0.43	0.45	71.82
Mean Annual Depth to Groundwater (in)	36.65	71.82	29024.32

(e)

Summary

The completeness of the data records for the USGS stations varied widely and hence some adjustments and data manipulation should be carried out to correct for any temporal discontinuities. This analysis data manipulation should include discarding some stations without monthly measurements for each of the representative years 2000-2004. Although analysis data manipulation did include the calculation of the mean and temporal trends for each USGS station, further temporal desegregation is needed in order to accurately represent the seasonality of the data (i.e. monthly not annual values).

The goal in trying to estimate groundwater level and withdrawal using variogram analysis and ordinary kriging was to identify two different types of correlations using product-moment calculations *(Pearson's r).* The first correlation was between the annual groundwater level and annual weighted groundwater withdrawal in Spring Creek Sub-basin Georgia. The second correlation pointed towards groundwater levels before and during hydrologic drought. This was accomplished by computing covariances for each year in the study period 2000 -2004. While this analysis could clearly define the relationship between groundwater levels and withdrawals, several observations were made about the performance of the data.

The usefulness of the data selected becomes evident in computing covariance calculations. In this analysis, three parameters are considered: Mean annual irrigation depth by year and county, mean annual groundwater level by depth and county and mean annual groundwater withdrawals by year and county. Stated earlier in the paper were the selection criteria for the USGS groundwater monitoring gages. Based on these criteria, Table 8 lists the number of observations available for each year of the study by county. It is clear that the year 2000 contains the highest number of groundwater measurements, between 10–15 monthly distributed observations. In 2001, 2002, and 2003 the range of available measurements are 5–12, 4 – 12, and 4–11, respectively. The decline in available data beginning in 2001 is most evident in 2004 with a range of available measurements 2 – 9, with an average of 6 measurements. This is why the covariance calculations show the strongest relationships between groundwater levels and withdrawals in 2000 and 2001 and do not perform as well from 2002 through 2004 (Table 9). On the other hand, covariance statistics between mean irrigation depth and groundwater withdrawals consistently show a strong dependency throughout the study period 2000-2004.

Table 9. Number of USGS groundwater observations by county and year.

County	Number of Observations [1999 2000 2001 2002 2003 2004]
Baker_A	[11 11 5 4 6 2]
Baker_B	[12 11 10 10 10 9]
Calhoun	[11 11 10 10 9 6]
Decatur_A	[12 10 12 7 9 7]
Decatur_B	[13 13 6 6 4 4]
Dougherty_A	[12 10 10 10 11 6]
Dougherty_B	[12 10 10 10 10 7]
Dougherty_C	[12 10 12 12 10 10 6]
Dougherty_D	[- 7 12 10 12 11]
Dougherty_E	[12 10 10 10 9 7]
Early	[12 14 8 4 4 3]
Lee	[16 12 6 3 4 3]
Miller_A	[12 15 8 6 5 5]
Miller_B	[11 11 10 11 10 7]
Mitchell_A	[13 12 10 10 10 7]
Mitchell_B	[13 13 8 5 4 3]
Worth	[13 11 11 11 11 12]

The spatial variogram analysis resulting in graduated color filled contour maps computed using ordinary kriging reveal a trend in both groundwater levels and withdrawals. The USGS stations that reflect the greatest impact in groundwater level fluctuations exhibit the highest response in groundwater irrigation withdrawals, though not quantifiable by any statistical measure. It was mentioned earlier that one of the goals of this study would be to determine if it would be possible to describe the interdependence between groundwater levels and groundwater withdrawals. In fact, this is a relationship that one would intuitively predict since the Upper Floridan aquifer exhibits connectivity to the surface water due to being an artesian aquifer composed of Carbonate-rock. However, if the covariance calculations are seen as the first indication that cross-covariance statistics would be strong, then I would have to say the future is bleak for this dataset. Later in the text we will look into this topic from another angle, the temporal variograms for groundwater levels in different counties.

Now we will compare two very different experimental temporal variograms and their corresponding groundwater level prediction models. Figures 29 (a) and (b) show a statistically valid (Table 10) experimental variogram model at Baker_A county for the observation period 2/5/1999 – 9/2/2004 with an average of 10.3 observations per year in a of sequence [12 11 10 10 10 9] for years 1999 - 2004 . The prediction model in this case shows the 95% confidence interval as a close band surrounding the observed groundwater levels. Similarly, Figures 20c and d show a statistically valid (Table 10) experimental variogram model at Lee county, but for the observation period 1/12/1999 – 9/8/2004 with an average of only 7.3 observations per year in a sequence of [16 12 6 3 4 3]. The groundwater level prediction model for Lee demonstrates how the number of observations can greatly influence the 95% confidence interval. Just as the number of observations drops after the 2nd year of the study period for Lee, the confidence interval balloons out after approximately the around the same time, yielding an inherently useless prediction model.

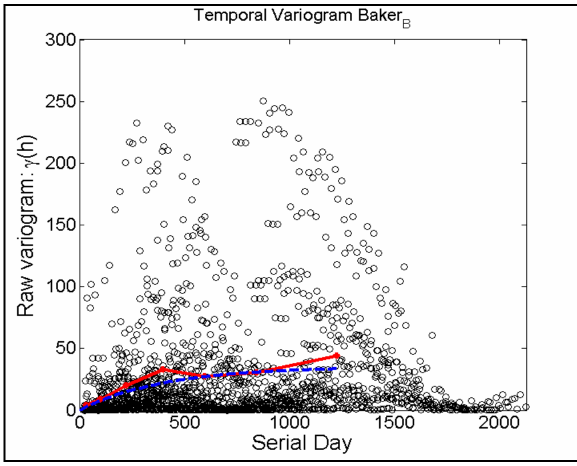

(a)

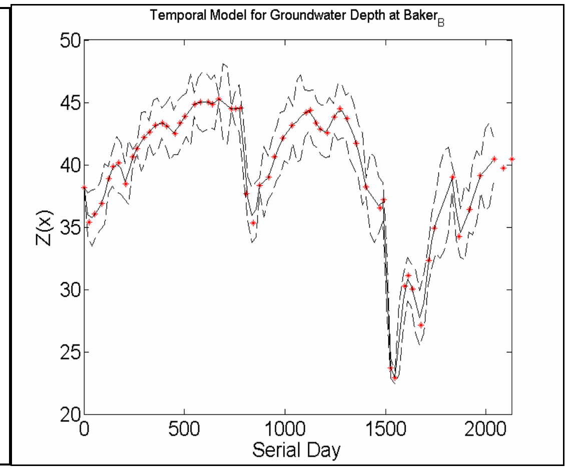

(b)

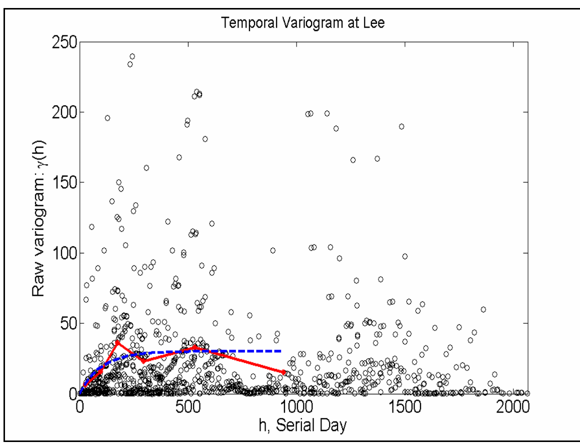

(c)

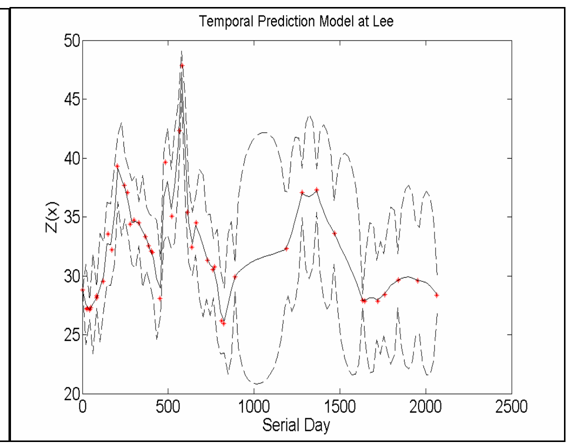

(d)

Figure 29. Temporal Variogram (a) and Prediction Model (b) for Groundwater level at Baker$_B$ for the observation period 2/5/1999 – 9/2/2004. . Temporal Variogram (c) and Prediction Model (d) for Groundwater level at Lee for the observation period 1/12/1999 – 9/8/2004.

Table 10. Experimental temporal variogram parameters and statistics for comparative analysis between a continuously monitored USGS site, Baker_B, and a sparsely monitored USGS site, Lee.

County	Validation Statistics			Exponential Model Parameters		Interval	Prediction Interval (Serial Value)		Prediction Interval (Convential Date)	
	Q1	**Q2**	**cR**	**Var**	**Length**	**Non-Uniform**	**tmin**	**tmax**	**tmin**	**tmax**
Lee	0.314	0.807	12.257	30	100	[50 150 200 400 700 1200]	0	2066	1/12/1999	9/8/2004
Baker_B	-0.029	1.266	5.447	35	400	[50 150 300 500 700 1000 1500]	0	2026	2/5/1999	9/2/2004

SUMMARY AND CONCLUSIONS

In this research, four research subtasks were completed: (1) spatial analysis of streamflow rate, groundwater level, and precipitation in the ACF river basin; (2) spatiotemporal analysis of precipitation; (3) spatiotemporal analysis of groundwater withdraw; and (4) a MATLAB geostatistical toolbox (see Appendix). The following conclusions may be drawn from the research tasks:

Geostatitical Theory

- The range of the optimal parameters of semi-variogram models is wider under the condition with 95% confidence than under the condition that Q_2 test is perfectly satisfied, but it is computationally efficient;
- Probabilistic forecast and potential map construction are accessible provided with accurate spatiotemporal analysis;
- A model decomposition in a spatiotemporal trend plus a residual should be associated with physical interpretations;
- Benchmark tests are necessary to test the optimization methods for estimating the best spatial correlation models and evaluate the forecasting results.

Field Application

- The magnitudes of correlation scales of groundwater levels, precipitations, groundwater withdraw, and streamflow rate are variable and different by orders in the ACF basin area;
- The spatial correlation ranges are 10.7, 0.4, and 25.5km for streamflow rate, groundwater level, and precipitation, respective, and for groundwater withdraw less than 1km, which indicating that groundwater withdraw and groundwater level have similar length scale in terms of spatial correlations
- Groundwater levels, groundwater withdraw, and precipitations are correlated and dependent;

- The covariance calculations show the strongest relationships between groundwater levels and withdrawals in 2000 and 2001 and do not perform as well from 2002 through 2004 (Table 9). On the other hand, covariance statistics between mean irrigation depth and groundwater withdrawals consistently show a strong dependency throughout the study period 2000-2004;

- The USGS stations that reflect the greatest impact in groundwater level fluctuations exhibit the highest response in groundwater irrigation withdrawals, though not quantifiable by any statistical measure;

- Although analysis data manipulation did include the calculation of the mean and temporal trends for each USGS station for groundwater withdraw, further temporal desegregation is needed in order to accurately represent the seasonality of the data (i.e. monthly not annual values).

SELECTED REFERENCES

Albertson, P.N., and L.J. Torak, Simulated effects of ground-water pumpage on stream-aquifer flow in the vicinity of federally protected species of freshwater mussels in the lower Apalachicola-Chattahoochee-Flint River basin (subarea 4), southeastern Alabama, northwestern Florida, and southwestern Georgia, U.S. Geological Survey Scientific Investigations Report 02-4016.

Bogaert, P., Comparison of kriging techniques in a space-time context, *Math. Geology*, *28*(1), 73–86, 1996.

Bras, R. L., and I. Rodrigues-Iturbe, Random functions and hydrology: Addison-Wesley,Reading, MA, 1984.

Cressie, N., Statistics for spatial data, John Wiley & Sons Inc., New York, 1993.

Cressie, N., and H.C. Huang, Classes of nonseparable, spatio-temporal stationary covariance functions, *Journal of the American Statistical Association 94*(448), 1330-1340, 1999.

Christakos, G., and P. Bogaert, Spatiotemporal analysis of spring water ion processes derived from measurements at the Dyle basin in Belgium, *IEEE Transactions on Geoscience and Remote Sensing*, *34*(3), 626–642, 1996.

Christakos, G., and R. Raghu, Dynamic stochastic estimation of physical variables, *Math. Geology*, *28*(3), 341–365, 1996.

Leeth, D.C., J.S. Clarke, C.J. Wipperfurth, and S.D. Craigg, Ground-Water Conditions and Studies in Georgia, 2002– 03, Scientific Investigations Report 2005-5065, 2005.

Warner, D., and J. Stephen. Lawrence Ground-Water Flow and Water Quality in the Upper Floridan Aquifer, Southwestern Albany Area, Georgia, 1998–2001 U.S. Geological Survey Scientific Investigations Report 2005-5047, 2005.

De Cesare, L., D.E. Myers, and D. Posa, Spatio-temporal modeling of $SO2$ in Milan district, *in* Baaffi, E., and Schofield, N., eds., Geostatistics Wollongong ’96, Vol. 2: Kluwer Academic Publ., Dordrecht, 1310–1042, 1997.

De Cesare, L., D.E. Myers, and D. Posa, Estimating and modeling space-time correlation structures, *Statistics & Probability Letters 51*, 9-14, 2001.

De Iaco, S., D.E. Myers, D. Posa, Space-time analysis using a general product-sum model. *Statistics & Probability Letters 52*, 21-28, 2001.

Dryden, I.L., L. Markus, C.C. Taylor, and J. Kovacs, Non-stationary spatiotemporal analysis of karst water levels, *Appl. Statist. 54*, 873-900, 2005.

Fanning, J.L., Water use in Georgia by county for 1995: Georgia Geologic Survey Information Circular 101, 1997.

Fanning, J.L., Water use in Georgia by county for 2000 and water-use trends for 1980 – 2000: Georgia Geologic Survey Information Circular 106, 2003.

Fuentes, M., L. Chen, J.M. Davis, and G.M. Lackmann, Modeling and predicting complex space-time structures and patterns of coastal wind fields, *Environmetrics*, *16*(5), 449-464, 2005.

Gneiting, T., Nonseparable, stationary covariance functions for space-time data, *JASA*, *97*, 590-600, 2002.

Georgia's Ground-Water Resources and Monitoring Network, U.S. Geological Survey Fact Sheet 2006-3077, 2006a.

Georgia's Surface-Water Resources and Streamflow Monitoring Network, U.S. Geological Survey Fact Sheet 2006-3084, 2006b.

Goovaerts, P., and C. Chiang, Temporal persistence of spatial patterns for mineralizable nitrogen and selected soil properties, *Soil Sci. Soc. America Jour.*, *57*(2), 372–381, 1993.

Haslett, J., Space time modeling in meteorology: A review, Proceedings of the 47th Session: International Statistical Institute, Paris, 229–246, 1989.

Haas, T. C., Statistical assessment of spatio-temporal pollutant trends and meteorological transport models, *Atmosph. Environment*, *32*(11), 1865–1879, 1998.

Hudson, G., and H. Wackernagel, Mapping temperature using kriging with external drift: Theory and an example from Scotland, *Int. Jour. Climatology*, *14*(1), 77–91, 1994.

Jones, R. H., and Y. Zhang, Models for continuous stationary space-time processes, in Gregoire, T. G., Brillinger, D. R., Diggle, P. J., Russek-Cohen, E., Warren, W. G., and Wolfinger, R. D., eds., Modelling longitudinal and spatially correlated data, Lecture Notes in Statistics, Vol. 122: Springer-Verlag, New York, p. 289–298, 1997.

Kirchner, J.W., X. Feng, and C. Neal, Fractal stream chemistry and its implications for contaminant transport in catchments, *Nature*, *403*, 524-527, 2000.

Kitanidis, P.K., Introduction to geostatistics: Applications in hydrogeology, Cambridge University Press, New York, 1997.

Klemes, V., The Hurst Phenomenon: A puzzle?, *Water Resour. Res.*, *10*, 675-688, 1974.

Kyriakidia, P.C., and A.G. Journel, Geostatistical space-time models: a review, *Math. Geology*, *31*(6), 61-684, 1999.

Mosner, M.S. Stream-aquifer relations and the potentiometric surface of the upper Floridan aquifer in the lower Apalachicola-Chattahoochee-Flint River basin in parts of Georgia, Florida, and Alabama, 1999-2000, U.S. Geological Survey Investigations Report 02-4244.

Myers, D. E., and A.G. Journel, Variograms with zonal anisotropies and noninvertible kriging systems: *Math. Geology*, *22*(7), 779–785, 1990.

Pereira, M. J., A. Soares, and C. Branquinho, Stochastic simulation of fugitive dust emissions, *in* Baaffi, E., and Schofield, N., eds., Geostatistics Wollongong'96, Vol. 2: Kluwer Academic Publ., Dordrecht, 1055–1065, 1997.

Rodriguez-Iturbe, I., and J.M. Mejia, The design of rainfall networks in time and space, *Water Resources Res.*, *10*(4), 713–728, 1974.

Rouhani, S., and D.E. Myers, Problems in space-time kriging of geohydrological data, *Math. Geology*, *22*(5), 611–623, 1990.

Simard, Y., and D. Marcotte, Assessing similarities and differences among maps: A study of temporal changes in distribution of northern shrimp (pandalus borealis) in the gulf of St. Lawrence, *in* A. Soares, ed., Geostatistics Tro´ ia '92, Vol. 2: Kluwer Academic Publ., Dordrecht, 865–874, 1993.

Skoien, J.O., G. Bloschl, and A.W. Western, Characteristic space scales and timescales in hydrology, *Water. Resour. Res*. *39*(10), 1304, doi:10.1029/2002WR001736, 2003.

Solna, K., and P. Switzer, Time trend estimation for a geographic region, *Jour. Am. Statistical Assoc.*, *91*(434), 577–589, 1996.

Stein, M.L., Space-time covariance functions. Tech. Report, University of Chicago, 2003.

Tabios, G., and J. Salas, A comparative analysis of techniques for spatial interpolation of precipitation, *Water Resources Bull.*, *21*(3), 365–380, 1985.

Torak, L.J., Physical and hydrochemical evidence of surface-water/ground-water mixing in and near Lake Seminole, southwestern Georgia and northwestern Florida: Proceedings of the 2001 Georgia Water Resources Conference, Athens, Georgia, Kathryn J. Hatcher, editor, 2001.

Torak, L.J., G.S. Davis, G.A. Strain, and J.G. Herndon, Geohydrology and evaluation of water-resource potential of the Upper Floridan aquifer in the Albany area, southwestern Georgia: U.S. Geological Survey Water-Supply Paper 2391, 1993.

Torak, L.J., G.S. Davis, G.A. Strain, and J.G. Herndon, Geohydrology and evaluation of stream-aquifer relations in the Apalachicola–Chattahoochee–Flint River Basin, southeastern Alabama, northwestern Florida, and southwestern Georgia: U.S. Geological Survey Water-Supply Paper 2460, 1996.

Torak, L.J., and R.J. McDowell, Ground-water resources of the lower Apalachicola – Chattahoochee – Flint River Basin in parts of Alabama, Florida, and Georgia – *Subarea* 4 of the Apalachicola – Chattahoochee – Flint and Alabama – Coosa– Tallapoosa River Basins: U.S. Geological Survey Open-File Report 95-321, 1996.

Torak, L.J., and J.A. Painter, Geohydrology of the lower Apalachicola-Chattahoochee-Flint River basin, southwestern Georgia, northwestern Florida, and southeastern Alabama, U.S. Geological Survey Scientific Investigations Report 2006-5070, 2006.

Venkatram, A., On the use of kriging in the spatial analysis of acid precipitation data, *Atmosph. Environment*, *22*(9), 1963–1975, 1988.

Wackernagel, H., Multivariate geostatistics: an introduction with applications, springer, Berlin, 1995.

APPENDIX – Geostatistical Analysis MATLAB Toolbox

Function - GeoKriging

```
function GeoKriging(filename, dim)
% Isotropic Ordinary Kriging System
% This program includes:
%    1. Expriment Variogram
%    2. Prelimanary selection of variogram model
%    3. Validation of variogram model
%    4. Prediction by ordinary kriging
% INPUT PARAMETER:
%   filename: INPUT FILE
%       Format of input data:
%            Measurement   Coordinates
%       For example:
%            Measurement   x   y   z
%   dim: dimension of data (1 - 1D; 2 - 2D; 3-3D)
%
% Jian Luo
% Georgia Institute of Technology
% Feb. 27, 2007

warning off;
fid = fopen(filename,'r');
% Reading input file
n = 1; huhu=fgets(fid); % the first line is a description line
switch dim
    case 1
        while 1
            data_in = fgetl(fid); if ~ischar(data_in), break, end
            [value(n),xyz(n,1)]=strread(data_in,'%f%f'); n = n+1;
        end
    case 2
        while 1
            data_in = fgetl(fid); if ~ischar(data_in), break, end
            [value(n),xyz(n,1),xyz(n,2)]=strread(data_in,'%f%f%f'); n =
n+1;
        end
    case 3
        while 1
            data_in = fgetl(fid); if ~ischar(data_in), break, end

[value(n),xyz(n,1),xyz(n,2),xyz(n,3)]=strread(data_in,'%f%f%f%f'); n =
n+1;
        end
end
fclose(fid);


% Number of measurements
Nmeas = length(value);

% Exprimental variogram
[hEff, expVario] = Exp_vario(filename, dim);
```

```
% Preliminary selection of variogram model
model_pre = 0; model_valid = 0;
xd = linspace(0, max(hEff));
while model_valid == 0
    while model_pre == 0
        disp('===============Preliminary Variogram Model Selection
============');
        disp('Please select the behavior near the origin:');
        Orig = input('1 --- No Nugget;   2 --- Nugget:   ');
        Station = input('Please select 1 --- Stationary;   2 ---
Nonstationary:   ');
        Nugget = 0;
        if Orig == 2
            Nugget = input('Please input the nugget value:  ');
        end
        if Station == 1
            model = input('Please select 1 --- Gaussian;   2 ---
Exponential:   ');
            sigma2 = input('Parameters (sigma2) = ');
            L      = input('Parameters    L     = ');
            Para = [sigma2 L];
            if model == 1
                vario = sigma2*(1-exp(-xd.^2/L^2));
            else
                vario = sigma2*(1-exp(-xd/L));
            end
        else
            model = 0;
            theta = input('Power Model Parameters (theta) = ');
            s     = input('Power Model Parameters (order) = ');
            Para = [theta s];
            vario = theta*xd.^s;
        end
        vario = vario + Nugget;
        figure(1001); hold on;
        plot(xd, vario, 'b--');
        model_pre = input('Do you want to try another type of model? 0
--- Yes; 1 --- No: ');
    end
    model_pre = 0;
% Model Validataion
    disp('=========================Model
Validation======================');
    delta(1)= value(2)-value(1);
    h1      = norm(xyz(1,:)-xyz(2,:));
    Kvar(1) =  gamma_vario(Nugget, Station, model, Para, h1);
    for np = 2:Nmeas-1
        A = zeros(np+1,np+1); b = zeros(np+1,1); % initialization
        [A, b] = OK_Ab(Nugget, Station, model, Para, xyz(1:np,:),
xyz(np+1,:));
        coef = A\b;
        ze = value(1:np)*coef(1:np);
        delta(np) = value(np+1)-ze;
        Kvar(np)  = -b'*coef;
    end
    Nres  = delta./sqrt(Kvar);
```

```
% Q1 and Q2 statistic
    Q1 = mean(Nres);
    Q2 = mean(Nres.^2);
    cR = exp(mean(log(Kvar)));

    Q1_r = 2/sqrt(Nmeas-1);
    Q2_r = 2.8/sqrt(Nmeas-1);
    disp(['Q1 = ', num2str(Q1)]);
    disp(['Q2 = ', num2str(Q2)]);
    disp(['cR = ', num2str(cR)]);

    if abs(Q1) > Q1_r & abs(Q2-1) > Q2_r
        disp('Both Q1 and Q2 statistic failed. The variogram model
should be rejected.');
    elseif abs(Q1) > Q1_r & abs(Q2-1) <= Q2_r
        disp('Q1 statistic failed. The variogram model should be
rejected.');
    elseif abs(Q1) <= Q1_r & abs(Q2-1) > Q2_r
        disp('Q2 statistic failed. The variogram model should be
rejected.');
    else
        disp('Congratulations! Both Q1 and Q2 statistic passed !!');
        model_valid = 1;
        if Station == 1 & model == 1
            disp(['The variogram model is a Gaussian model: variance =
', num2str(sigma2), ' and L = ',num2str(L),...
                ' and Nugget = ',num2str(Nugget)]);
        elseif Station == 1 & model == 2
            disp(['The variogram model is a Exponential model: variance
= ', num2str(sigma2), ' and L = ',num2str(L),...
                ' and Nugget = ',num2str(Nugget)]);
        elseif Station == 2
            disp(['The variogram model is a Power model: theta = ',
num2str(theta), ' and order = ', num2str(s),...
                'and Nugget = ',num2str(Nugget)]);
        end

disp('=================================================================
=================');
        cont = input('Do you want to use the variogram model for
prediction? 1 --- Yes; 2 --- No: ');
        if cont == 1
            switch dim
                case 1
                    xmin = input('Minimum x: ');
                    xmax = input('Maximum x: ');
                    dx   = (xmax-xmin)/100;
                    xp   = xmin:dx:xmax;
                    Ap = OK_A(Nugget, Station, model, Para, xyz, dim);
                    bp = OK_b(Nugget, Station, model, Para, xyz, xp',
dim);
                    coef_p = Ap\bp;
                    zp = value*coef_p(1:end-1,:);
                    zp_var  = diag(-coef_p'*bp);
                    figure(1002)
```

```
                    plot(xyz, value, 'r*'); hold on;
                    plot(xp', zp, 'k-');
                    plot(xp', zp+2*sqrt(zp_var'), 'k--');
                    plot(xp', zp-2*sqrt(zp_var'), 'k--');
                    xlabel('x','fontsize',20);
ylabel('Z(x)','fontsize',20);
                    set(gca,'fontsize',20);
                case 2
                    xmin = input('Minimum x: ');
                    xmax = input('Maximum x: ');
                    dx   = (xmax-xmin)/50;
                    ymin = input('Minimum y: ');
                    ymax = input('Maximum y: ');
                    dy   = (xmax-xmin)/50;
                    xp   = xmin:dx:xmax;
                    yp   = ymin:dy:ymax;
                    [XP, YP] = meshgrid(xp,yp);
                    [k1, k2] = size(XP);
                    zp   = [reshape(XP, k1*k2,1) reshape(YP, k1*k2,1)];
                    Ap = OK_A(Nugget, Station, model, Para, xyz, dim);
                    bp = OK_b(Nugget, Station, model, Para, xyz, zp,
dim);
                    coef_p = Ap\bp;
                    ze = value*coef_p(1:end-1,:);
                    ze = reshape(ze, k1,k2);
                    ze_var  = -coef_p'*bp;
                    ze_v = diag(ze_var);
                    ze_v = reshape(ze_v, k1,k2);
                    figure(1002)
                    pcolor(XP,YP,ze); shading interp; colorbar vert;
hold on;
                    [C,Hand] = contour(XP,YP,ze);
                    text_handle = clabel(C,Hand);
                    set(text_handle,'BackgroundColor',[1 1 .6],...
                        'Edgecolor',[.7 .7 .7]);
                    set(Hand,'linewidth',2,'linecolor','k');
                    xlabel('x','fontsize',20);
ylabel('y','fontsize',20);
                    set(gca, 'fontsize',20);
                    title('Krigged Z(x,y)');
                    figure(1003)
                    pcolor(XP,YP,ze_v); shading interp; colorbar vert;
hold on;
                    [C,Hand] = contour(XP,YP,ze_v);
                    text_handle = clabel(C,Hand);
                    set(text_handle,'BackgroundColor',[1 1 .6],...
                         'Edgecolor',[.7 .7 .7]);
                    set(Hand,'linewidth',2,'linecolor','k');
                    xlabel('x','fontsize',20);
ylabel('y','fontsize',20);
                    set(gca, 'fontsize',20);
                    title('Variance');
                case 3
                    nxyz = 20;
                    xmin = input('Minimum x: ');
                    xmax = input('Maximum x: ');
                    dx   = (xmax-xmin)/nxyz;
```

```
                    ymin = input('Minimum y: ');
                    ymax = input('Maximum y: ');
                    dy   = (ymax-ymin)/nxyz;
                    zmin = input('Minimum z: ');
                    zmax = input('Maximum z: ');
                    dz   = (zmax-zmin)/nxyz;
                    xv   = xmin:dx:xmax;
                    yv   = ymin:dy:ymax;
                    zv   = zmin:dz:zmax;
                    [XV,YV,ZV] = meshgrid(xv,yv,zv);
                    [k1,k2,k3] = size(XP);
                    zp   = [reshape(XV, k1*k2*k3,1) reshape(YV,
k1*k2*k3,1) reshape(ZV, k1*k2*k3,1)];
                    Ap = OK_A(Nugget, Station, model, Para, xyz, dim);
                    bp = OK_b(Nugget, Station, model, Para, xyz, zp,
dim);
                    coef_p = Ap\bp;
                    ze = value*coef_p(1:end-1,:);
                    ze = reshape(ze, k1,k2,k3);
                    ze_var  = -coef_p'*bp;
                    ze_v = diag(ze_var);
                    ze_v = reshape(ze_v, k1,k2,k3);
                    figure(1002)
                    xs1 = mean(10); xs2 = max(20);
                    ys1 = yv(5); ys2 = yv(15);
                    zs1 = zv(3); zs2 = zv(20);
                    slice(XV,YV,ZV,ze,[xs1 xs2],[ys1 ys2],[zs1 zs2]);
                    h = contourslice(XV,YV,ZV,ze, xs2, [ys1 ys2], []);
                    set(h,'EdgeColor','k','Linewidth',1.5);
                    xlabel('X-axis');
                    ylabel('Y-axis');
                    zlabel('Z-zxis');
                    title('Krigged Z(x,y,z)');
                    figure(1003)
                    xs1 = mean(10); xs2 = max(20);
                    ys1 = yv(5); ys2 = yv(15);
                    zs1 = zv(3); zs2 = zv(20);
                    slice(XV,YV,ZV,ze_var,[xs1 xs2],[ys1 ys2],[zs1
zs2]);
                    h = contourslice(XV,YV,ZV,ze_v, xs2, [ys1 ys2], []);
                    set(h,'EdgeColor','k','Linewidth',1.5);
                    xlabel('X-axis');
                    ylabel('Y-axis');
                    zlabel('Z-zxis');
                    title('Variance');
            end
        end
    end
end
```

Function – Exp_vario

```
function [hEff,expVario] = Exp_vario(filename, dim)
% Exp_vario - calculate the experimental variogram
%
% DESCRIPTION:
%   This function calculates the raw variogram and experimental
variogram.
% INPUT PARAMETER:
%   filename: INPUT FILE
%       Format of input data:
%            Measurement   Coordinates
%       For example:
%            Measurement   x   y   z
%   dim: dimension of data (1 - 1D; 2 - 2D; 3-3D)
%
% Jian Luo
% Georgia Institute of Technology
% Feb. 27, 2007

fid = fopen(filename,'r');
% Reading input file
n = 1; huhu=fgets(fid); % the first line is a description line
switch dim
    case 1
        while 1
            data_in = fgetl(fid); if ~ischar(data_in), break, end
            [value(n),x(n)]=strread(data_in,'%f%f'); n = n+1;
        end
    case 2
        while 1
            data_in = fgetl(fid); if ~ischar(data_in), break, end
            [value(n),x(n),y(n)]=strread(data_in,'%f%f%f'); n = n+1;
        end
    case 3
        while 1
            data_in = fgetl(fid); if ~ischar(data_in), break, end
            [value(n),x(n),y(n),z(n)]=strread(data_in,'%f%f%f%f'); n =
n+1;
        end
end
fclose(fid);

% Raw Vaiogram
ndata = length(value);
m = 1;
for a = 1:ndata-1
    for b = a+1:ndata
        rawVario(m) = 1/2*(value(a)-value(b))^2;
        switch dim
            case 1
                hRaw(m)     = abs(x(a)-x(b));
            case 2
                hRaw(m)     = sqrt((x(a)-x(b))^2+(y(a)-y(b))^2);
            case 3
                hRaw(m)     = sqrt((x(a)-x(b))^2+(y(a)-y(b))^2+(z(a)-
z(b))^2);
```

```
        end
        m = m+1;
    end
end

% Plotting raw variogram
figure(1001)
plot(hRaw, rawVario, 'ko'); hold on;
xlabel('h','fontsize',20);
ylabel('Raw variogram: \gamma(h)','fontsize',20);
set(gca,'fontsize',20);
xlim([0 max(hRaw)+1]);
drawnow;

% Experimental Variogram
disp('==================Experimental Variogram
======================');
uniform   = input('Uniform (0) or nonuniform (1) intervals for the
experiment variogram: ');
switch uniform
    case 0
        ninterval = input('How many intervals for the experimental
variogram:  ');
        maxh      = ceil(max(hRaw));
        hk        = 0:maxh/ninterval:maxh;

    case 1
        hk    = input('Please input your discretization as a vector:
');
        hk    = [0 hk];
end

nhk = length(hk);
for nm = 1:nhk-1
    ihk = find(hRaw >= hk(nm) & hRaw < hk(nm+1));
    expVario(nm) = mean(rawVario(ihk));
    hEff(nm) = mean(hRaw(ihk));
end

% Plotting experimental variogram
plot(hEff, expVario, 'r*-');
```

Function – gamma_vario

```
function huhu = gamma_vario(Nugget, Station, model, para, dis)
% This function returns the variogram calculation.
% Models: Gaussian, Exponential, and Power, w/o Nugget
if Station == 1 & model == 1
    sigma2 = para(1); L = para(2);
    huhu = Nugget + sigma2*(1-exp(-dis.^2/L^2));
elseif Station == 1 & model == 2
    sigma2 = para(1); L = para(2);
    huhu = Nugget + sigma2*(1-exp(-dis/L));
elseif Station == 2
    theta = para(1); s = para(2);
    huhu = Nugget + theta*dis.^s;
end
```

Function – OK_A

```
function Am = OK_A(Nugget, Station, model, Para, coordinate, dim)
% Organizing Matrix A and b for Ordinary Kriging
xyz = coordinate;
np = size(coordinate,1);

switch dim
    case 1
        h = abs(repmat(xyz,1,np)-repmat(xyz',np,1));
    case 2
        X = xyz(:,1); Y = xyz(:,2);
        h1 = abs(repmat(X,1,np)-repmat(X',np,1));
        h2 = abs(repmat(Y,1,np)-repmat(Y',np,1));
        h  = sqrt(h1.^2+h2.^2);
    case 3
        X = xyz(:,1); Y = xyz(:,2); Z = xyz(:,3);
        h1 = abs(repmat(X,1,np)-repmat(X',np,1));
        h2 = abs(repmat(Y,1,np)-repmat(Y',np,1));
        h3 = abs(repmat(Z,1,np)-repmat(Z',np,1));
        h  = sqrt(h1.^2+h2.^2+h3.^2);
end
Am = -gamma_vario(Nugget, Station, model, Para, h).*(h~=0);
Am = [Am ones(np,1); ones(1,np) 0];
```

Function – OK_Ab

```
    function [Am, bm] = OK_Ab(Nugget, Station, model, Para, coordinate,
xyz0)
    % Organizing Matrix A and b for Ordinary Kriging
    xyz = coordinate;
    np = size(coordinate,1);
    Am = zeros(np+1,np+1); bm = ones(np+1,1); % initialization
    for row = 1:np
        Am(row,row) = 0;
        for col = row+1:np
            h = norm(xyz(row,:)-xyz(col,:));
            Am(row,col) = -gamma_vario(Nugget, Station, model, Para,
h)*(h~=0);
            Am(col,row) = Am(row,col);
        end
        Am(row,np+1) = 1; Am(np+1,row) = 1;
        h = norm(xyz(row,:)-xyz0);
        bm(row,1) = -gamma_vario(Nugget, Station, model, Para,
h)*(h~=0);
    end
```

Function – OK_b

```
function bm = OK_b(Nugget, Station, model, Para, coordinate, xyz0,
dim)
% Organizing Matrix A and b for Ordinary Kriging
nx0 = length(xyz0);
xyz = coordinate;
np = size(coordinate,1);
switch dim
    case 1
        h = abs(repmat(xyz,1,nx0)-repmat(xyz0',np,1));
    case 2
        X = xyz(:,1); Y = xyz(:,2);
        X0 = xyz0(:,1); Y0 = xyz0(:,2);
        h1 = abs(repmat(X,1,nx0)-repmat(X0',np,1));
        h2 = abs(repmat(Y,1,nx0)-repmat(Y0',np,1));
        h  = sqrt(h1.^2+h2.^2);
    case 3
        X = xyz(:,1); Y = xyz(:,2); Z = xyz(:,3);
        X0 = xyz0(:,1); Y0 = xyz0(:,2); Z0 = xyz0(:,3);
        h1 = abs(repmat(X,1,nx0)-repmat(X0',np,1));
        h2 = abs(repmat(Y,1,nx0)-repmat(Y0',np,1));
        h3 = abs(repmat(Z,1,nx0)-repmat(Z0',np,1));
        h  = sqrt(h1.^2+h2.^2+h3.^2);
end
bm = -gamma_vario(Nugget, Station, model, Para, h).*(h~=0);
bm = [bm; ones(1, nx0)];
```